Microbiological Research 306 (2026) 128442

Contents lists available at ScienceDirect

Microbiological Research

journal homepage: www.elsevier.com/locate/micres

Automated high-throughput microscopy screening unveiled new *Listeria monocytogenes* genes involved in cell infection

Ângela Alves [a,b,c], Diana Meireles [a,b,c], Chiara Suriano [a,b], Ricardo Monteiro [a,b], Rute Oliveira [a], Beatriz G. Bernardes [d], Sandra Sousa [a,b], Rita Pombinho [a,b], Didier Cabanes [a,b,*]

[a] Instituto de Investigação e Inovação em Saúde - i3S, Universidade do Porto, Portugal
[b] Instituto de Biologia Molecular e Celular - IBMC, Porto, Portugal
[c] McBiology Doctoral Program, Instituto de Ciências Biomédicas Abel Salazar - ICBAS, Universidade do Porto, Portugal
[d] Universidade Católica Portuguesa, CBQF - Centro de Biotecnologia e Química Fina – Laboratório Associado, Escola Superior de Biotecnologia, Porto, Portugal

ARTICLE INFO

Keywords:
Automated high-throughput microscopy
Listeria monocytogenes
Cell infection
PurA
GAPDH

ABSTRACT

To uncover novel genetic factors required for *Listeria monocytogenes* cell infection, we developed an automated high-throughput microscopy screening pipeline that integrates GFP-expressing *bacteria* with machine learning-based image analysis. Using this approach, we screened a mariner transposon library comprising 4224 *L. monocytogenes* EGDe mutants and identified 58 with significantly reduced numbers of intracellular bacteria. Sequencing revealed 24 unique insertion sites corresponding to 14 genes, including previously known virulence factors and nine novel candidates not previously implicated in cell infection. These genes encode the protease chaperone ClpX, the ferric uptake regulator Fur, the sensor histidine kinase LisK, the peptide chain release factor 2 PrfB, proteins involved in proline and purine biosynthesis (ProAB, PurAB), and Lmo2217, a protein of unknown function. Among these, the targeted deletion of the adenylosuccinate synthetase gene, *purA*, resulted in impaired growth in minimal medium, severely reduced proliferation in epithelial and macrophage cell lines, and attenuated virulence in mice. Unexpectedly, PurA was also essential for bacterial internalization into cells. Supplementation with AMP or adenine, but not ATP, rescued the invasion capacity of the Δ*purA* mutant. Mechanistically, *purA* deletion induced a reduction in the levels of surface-associated GAPDH, a putative plasminogen-binding protein, likely contributing to the observed invasion defect. Overall, these findings highlight the power of automated high-throughput microscopy screening to dissect host–pathogen interactions, identify novel *L. monocytogenes* genes required for cell infection, and uncover an unexpected role for PurA in maintaining GAPDH surface localization and promoting bacterial entry into host cells.

1. Introduction

Listeriosis is one of the most severe food-borne illnesses under EU surveillance, due to the high rate of hospitalizations, elevated morbidity and mortality, particularly among immunocompromised individuals, pregnant women and the elderly (Food Safety Authority, Center for Disease Prevention, 2024). *Listeria monocytogenes*, the causative agent of listeriosis, is a facultative intracellular pathogen with a remarkable ability to invade, survive and proliferate within different host cell types and tissues, and evade immune responses (Radoshevich and Cossart, 2017). The success of this Gram-positive pathogen results in particular from its ability to promote its own internalization by non-phagocytic cells, which enables the bacterium to overcome important pathophysiological barriers, such as the intestinal epithelium, the blood-brain barrier and the placenta (Cossart, 2011). To efficiently infect cells, *L. monocytogenes* makes use of a large array of virulence effectors (Schlech, 2019). Bacteria first adhere to host cells using several adhesins, including the amidase Ami (Jonquières et al., 1999). Bacterial entry into cells is then induced by the interaction of the two principal surface invasins, InlA and InlB, with their specific host cell receptors (Dramsi et al., 1995; Gaillard et al., 1991). *L. monocytogenes* is engulfed in a vacuole, which is rapidly lysed by the concerted action of listeriolysin O (LLO) and phospholipases C (PI-PLC and PC-PLC) (Osanai et al., 2013; Smith et al., 1995), allowing vacuole escape and replication in the cell cytosol, using glucose-1-phosphate through the activity of the hexose phosphate transporter Hpt (Chico-Calero et al., 2002; Ray et al.,

* Corresponding author at: Instituto de Investigação e Inovação em Saúde - i3S, Universidade do Porto, Portugal
E-mail address: didier@i3s.up.pt (D. Cabanes).

https://doi.org/10.1016/j.micres.2026.128442
Received 29 September 2025; Received in revised form 8 January 2026; Accepted 10 January 2026
Available online 13 January 2026

2009). Bacterial surface protein ActA polymerizes host actin, promoting cell-to-cell spread (Pillich et al., 2017). Although many *L. monocytogenes* virulence factors have been described, the function of at least 30 % of its genes remains unknown. To address this issue, efficient high-throughput assays are now necessary.

A powerful approach to unravel new genes involved in bacterial cellular infection is mutagenesis screening using transposons like *Himar1*, a widespread transposable element suitable for transposition of low-GC-content bacteria, such as *L. monocytogenes* (Lampe et al., 1996). Transposon mutant libraries have been widely used to identify *L. monocytogenes* genes involved in adaptation to environmental factors, stress response mechanisms, resistance to antimicrobials (Guerreiro et al., 2020a; Narayanan et al., 2022; Nowak et al., 2021; Pang et al., 2022; Parsons et al., 2017; Paspaliari et al., 2017), adhesion to host cells (Milohanic et al., 2000), and intracellular replication (Fischer et al., 2022; Schauer et al., 2010). Typically, the *L. monocytogenes* cell infection process is assessed by gentamicin survival and plaque formation assays, or direct microscopy. However, these techniques are time-consuming and unsuitable for large-scale screens. Integrative plasmids encoding fluorescent proteins were developed to easily, rapidly, and quantitatively detect intracellular *L. monocytogenes* (Balestrino et al., 2010) and automated fluorescence microscopy-based imaging methods allow high-throughput analysis of cell infection (Agaisse et al., 2005).

In this study, we coupled chromosomally tagged fluorescent *L. monocytogenes* and automated high-throughput microscopy to screen a genome-wide *mariner*-based transposon library and unveiled new genes involved in cell infection.

2. Materials and methods

2.1. Bacterial strains, plasmids, cell lines and growth conditions

Strains and plasmids used in this study are detailed in Supplementary Table S1. *Listeria monocytogenes* and *Escherichia coli* strains were routinely cultured in Brain Heart Infusion (BHI, Difco) and Lysogeny Broth (LB, Difco) broth, respectively, at 37 °C with agitation (200 rpm). *Listeria* strains constitutively and stably expressing a fluorescent GFP protein were cultured in the presence of chloramphenicol (Cm) 7 or 7.5 μg/ml. When appropriate, antibiotics were added as selective agents at the following concentrations: ampicillin (Amp) 100 μg/ml, erythromycin (Ery) 1 or 5 μg/ml and kanamycin (Kan) 50 μg/ml. For genetic complementation, colistin sulfate (Col) and nalidixic acid (Nax) were used at 10 and 50 μg/ml, respectively.

Human colorectal adenocarcinoma cell line CaCo-2 (ATCC HTB-37) was propagated in Eagle's medium with L-glutamine (EMEM, Lonza), supplemented with 20 % Fetal Bovine Serum (FBS, Biowest), 0.1 mM non-essential amino acids (Lonza) and 1 mM sodium pyruvate (Lonza). Human choriocarcinoma cell line Jeg-3 (ATCC HTB-36) was cultured under similar conditions but with 10 % FBS. Human cervical adenocarcinoma cell line HeLa (ATTC CCL-2) and RAW 264.7 cells (ATTC TIB-71) were grown in Dulbecco's modified Eagle's medium (DMEM) with glucose (4.5 g/l) and L-glutamine (Lonza) supplemented with 10 % FBS. Cells were maintained at 37 °C in a 5 % CO_2 humidified atmosphere.

2.2. Generation of L. monocytogenes transposon mutant library

To generate the *L. monocytogenes* EGDe::pIMK-cGFP strain, the GFP, along with its upstream regulatory region, was amplified by PCR (Table S2), using the pAD-cGFP plasmid as a template (Balestrino et al., 2010). The PCR fragment was then digested and ligated into the digested pIMK vector (Monk et al., 2008). Using light microscopy, we confirmed that the bacteria were successfully expressing GFP. Electrocompetent *L. monocytogenes* EGDe::pIMK-cGFP was prepared as previously described (Park and Stewart, 1990), with a slight modification to increase electroporation efficiency. Briefly, *L. monocytogenes* EGDe::pIMK-cGFP was inoculated in Veggie-Sucrose medium (Veggie Peptone broth (OXOID) supplemented with 0.5 M sucrose) until reached mid-log phase. Penicillin G was added to the culture, which grew for 2 h ($OD_{600\ nm} = 1$). Pelleted bacteria were resuspended in HEPES-Sucrose (10 ml) and incubated with lysozyme (100 μg/ml) for 20 min at 37 ºC. Treated-pelleted bacteria were washed twice and resuspended in 200 μl of HEPES-Sucrose to be aliquoted. A highly pure and concentrated pJZ037 plasmid was obtained by midi-prep. For electroporation, 2 μg of plasmid was mixed with 50 μl of competent cells. After 5 min on ice, the mixture was added to a 0.1 cm cuvette and electroporated (1 KV, 400 ohms, 25 μFD). Bacteria were recovered in Veggie-Sucrose medium during 2 h at 30 ºC, plated on BHI containing chloramphenicol 7.5 μg/ml, and incubated at 30 ºC for 4 days. Grown colonies were scraped and mixed into Phosphate-Buffered Saline (PBS, Lonza), washed, diluted, plated in BHI supplemented with Ery 1 μg/ml, and incubated at 42 ºC. Grown colonies were picked individually to replicate in BHI Ery (1 μg/ml) and BHI Cm (7.5 μg/ml). The transposon mutant library is composed by all the bacteria that grew in the presence of Ery but not in the presence of Cm (Rate of plasmid retention obtained = 4.9). All the transposon mutants were inoculated in 200 μl of BHI, in 96-well plates and incubated overnight at 37 ºC with agitation. The following day, the library was frozen, in duplicate, at −80 ºC. Randomness of the library was tested by sending 50 transposon mutants for sequencing analysis.

2.3. Transposon mutant screen for genes involved in the L. monocytogenes intracellular lifecycle

The day before the assay, 4224 transposon mutants of *L. monocytogenes* were inoculated (microplate replicator) in BHI and incubated overnight at 37 ºC with agitation in black 96-well microplates with clear flat-bottom (*L. monocytogenes* EGDe::pIMK-cGFP was included in each plate). HeLa cells were seeded (6×10^4 cells/well) in 96 well-plates (PerkinElmer, MA, USA) using an automated bulk dispenser (Multidrop Combi, ThermoScientific, MA, USA). In the following day, bacteria were washed, diluted in DMEM (1:10), and used to infect HeLa cells, using an automated liquid handling workstation (JANUS, PerkinElmer, MA, USA) (MOI 5). After 2 h, gentamicin (50 μg/ml) was added to the cells for 15 h. For the high-throughput screening, 17h-infected cells were washed twice with PBS, fixed in 4 % paraformaldehyde (PFA, Eletron Microscopy Sciences) (30 min, room temperature, in the dark), and washed again in PBS. *L. monocytogenes* stably expresses a fluorescent GFP protein, and the DNA was counterstained with DAPI (Sigma, 1:1000). Four representative images of each transposon-mutant infecting cells were collected with an automated widefield High Content Screening (HCS) microscope (IN Cell Analyzer 2000, GE Healthcare, IL, USA). Machine-learning-based bioimage analysis was done using predefined workflows for image segmentation, object classification and counting. Cell nuclei and bacteria were depicted in blue and green, respectively, and cell nuclei expansion was outlined (red) in the images. CellProfiler used the Ilastik-generated data to extract quantitative measurements from the automatically acquired images. The ratio of the number of bacteria per cell (bacteria/cell) for each transposon mutant was normalized to the bacteria-to-cell ratio of *L. monocytogenes* EGDe (ATCC-BAA-679) Wild Type (WT), set to 1. Mutants were identified as significant hits if their values fell below the WT average minus three times its standard deviation, ensuring a 99 % confidence level for selection.

2.4. Transposon-mutants sequencing

Sequential PCR reactions were performed to identify the junction of the transposon insertion into the *L. monocytogenes* genome. TnMAP1 reaction was performed using 1 μl of resuspended transposon-mutant colony, 12.5 μl of KAPA2G Fast ReadyMix, 1.25 μl of each primer (TN1, ARB1) and distilled water in a 25 μl reaction volume. The PCR cycling protocol was the following: 1 cycle at 95 ºC (300 s); 15 cycles at

98 ºC (10 s), 48 ºC (decrease of 1 ºC/cycle) (30 s), 72 ºC (180 s); 15 cycles at 98 ºC (10 s), 60 ºC (30 s), 72 ºC (120 s). Then, TnMAP2 reaction was performed using 1 µl of TnMAP1 PCR product as template, 12.5 µl of KAPA2G Fast ReadyMix, 1.25 µl of each primer (TN3, ARB2), and distilled water in a 25 µl reaction volume. The PCR cycling protocol was the following: 1 cycle at 95 ºC (30 s); 25 cycles at 98 ºC (10 s), 60 ºC (30 s), 72 ºC (60 s); 72 ºC (120 s). ExoSAP reaction was performed mixing 5 µl of TnMAP2 PCR product with 2 µl of ExoSAP-IT PCR Product Cleanup Reagent (ThermoFisher). The PCR cycling protocol was the following: 37 ºC (30 min); 80 ºC (20 min). TNSeq primer was added directly to ExoSAP-treated PCR product and sent for sequencing. Primers are listed in Supplementary Table S2.

2.5. Mutant construction and strain complementation

Gene deletion from the *L. monocytogenes* EGDe WT chromosome was achieved by double homologous recombination using the suicide plasmid pMAD (Arnaud et al., 2004). This procedure was previously described with details (Carvalho et al., 2015).

Complementation was achieved by genomic reintroduction of the gene *in trans*, as described before (Camejo et al., 2009), using a *L. monocytogenes* specific integrative plasmid pIMK (Monk et al., 2008). Primers are listed in Supplementary Table S2.

2.6. Growth analysis in vitro

Growth of *L. monocytogenes* strains was evaluated under different conditions. Overnight cultures were diluted 100-fold in fresh BHI broth, chemically defined minimal medium (MM), or MM supplemented with adenine (1 mM, Sigma-Aldrich), adenosine monophosphate (AMP, 1 mM, Thermo Fisher Scientific), or adenosine triphosphate (ATP, 1 mM, Sigma-Aldrich). The MM composition was previously described (Tsai and Hodgson, 2003). Cultures were incubated at 37 ºC with shaking, and growth was monitored by measuring the optical density at 600 nm overtime (Tsai and Hodgson, 2003).

2.7. Cell adhesion, invasion, and intracellular multiplication assays

Cell infections were performed as previously described (Reis et al., 2010). For adhesion assays, exponential-phase *L. monocytogenes* was washed and inoculated at a multiplicity of infection (MOI) of 50 for 30 min. Cells were washed three times with PBS and lysed with cold 0.1 % Triton X-100 (Sigma-Aldrich). Adherent bacteria were serially diluted and plated on BHI-agar plates for colony forming unit (CFU) quantification. For invasion and intracellular multiplication assays, bacteria were prepared as above and inoculated at MOI 50 or 5 for 1 or 2 h, respectively. Cells were then incubated with medium supplemented with 20 or 50 µg/ml gentamicin (Lonza) for 1.5 h or 15 h to eliminate extracellular bacteria, washed with PBS and lysed with cold 0.1 % Triton X-100. Intracellular bacteria were serially diluted and plated for CFU counting.

Assays of intracellular multiplication in mouse macrophages were performed as described (Reis et al., 2010). Cells were infected with exponential-phase bacteria at MOI 20 for 20 min and incubated with medium supplemented with 20 µg/ml of gentamicin. At 30 min, 1 h, 1.5 h, 2 h, 4 h, 6 h and 24 h post-infection, cells were washed three times with PBS and lysed with cold 0.1 % Triton X-100. Intracellular bacteria were diluted and quantified by CFU counting. Three independent assays were performed in triplicate.

Whenever indicated, either bacteria were supplemented with adenine or AMP (1 mM) immediately before cell infection, or cells were pre-treated with adenine or AMP (1 mM) for 1 h and washed before being infected. Cell assays were performed in three independent experiments.

2.8. Scanning electron microscopy (SEM)

Bacterial samples were harvested from different growth conditions during exponential growth and added to coverslips previously treated with Poly-L-Lysine (Sigma-Aldrich) for 1 h, at room temperature, to promote bacterial attachment. Samples were then washed twice with PBS and fixed for 1 h at room temperature (1.5 % glutaraldehyde (Sigma-Aldrich), 0.14 M sodium cacodylate (Sigma-Aldrich)). After fixation, the samples were rinsed twice with distilled water before being dehydrated in a graded ethanol series (50 %, 60 %, 70 %, 80 %, 90 %, and 99 %) for 10 min each and dried in a critical point dryer. Samples were mounted on observation stubs using double-sided adhesive carbon tape, sputter-coated with a 9 −12 nm layer of gold/palladium (Polaron) and acquired in a Phenom Pro G6 SEM (Thermo Fisher Scientific - FEI, MA, USA) at an accelerating voltage of 10 kV, with the Secondary Electron Detector (SED) and a magnification of 35,000×. Images were analysed and bacterial length was quantified using ImageJ software v1.5 f.

2.9. High performance liquid chromatography (HPLC) analysis

To measure extracellular AMP levels overtime, HeLa cells were washed with DMEM and incubated with DMEM supplemented with AMP (1 mM) for 1 h. At 5, 10, 20, 40, and 60 min, cell culture supernatants were collected, filtered through a ClearSpin filter (cellulose acetate membrane, 0.45 µm pore size), and centrifuged at 13000 rpm for 1 min at room temperature. AMP were quantified by HPLC system (Thermo Vanquish, MA, USA). Chromatographic separation of AMP was achieved using an analytical reverse phase column C18 (5 µm, 250 mm × 4 mm, Lichrospher®100) at 25 ºC. The best chromatographic conditions were obtained while using an isocratic program with a mobile phase composed of 50 mM phosphate buffer pH 7, 20 mM tetrabutylammonium bromide (TBAB) and 20 % methanol, a flow rate of 1 ml/min and 10 µL injection volume. The detection wavelength was set to 254 nm to retrieve the AMP retention time. Peak integration and data analysis were performed using Chromeleon™ Software v7.2.10.24543.

DMEM stock solution and standard solutions of AMP (0.1 mM, 0.2 mM, 0.4 mM, 0.8 mM, and 1 mM) were prepared to generate a calibration curve and validate HPLC analytical quantification.

2.10. Extraction of L. monocytogenes proteins

The extraction of surface-associated *L. monocytogenes* proteins was performed as previously described (Carvalho et al., 2018), with minor modifications. Exponential-phase bacteria (20 ml, $OD_{600\ nm}$~0.8) were harvested by centrifugation at 3800 g for 15 min at room temperature and the bacterial pellet was washed with DMEM. Bacteria were then incubated in DMEM or DMEM supplemented with AMP (1 mM) for 1 h at 37 °C with 5 % CO_2. Bacteria were pelleted by centrifugation, resuspended in PBS containing 2 % sodium dodecyl sulphate (SDS), and incubated for 30 min at 37 °C. Samples were centrifuged at 21,000 g for 1 min. Solubilized cell surface-bound proteins were collected for Western blot analysis.

2.11. SDS-PAGE and western blot analysis of protein extracts

Protein extracts from *L. monocytogenes* were resolved by SDS-PAGE in an 8 % polyacrylamide gel and transferred onto nitrocellulose membrane for 1 h in a TransBlot®Turbo System (BioRad Laboratories, CA, USA). Nitrocellulose membranes were stained with Ponceau S before blocking (5 % Bovine serum albumin (BSA, Sigma-Aldrich)) in Buffer A (20 mM Tris-HCl, 0.9 % NaCl, pH 7.4 and 0.1 % Tween 20), 1 h at room temperature. Membranes were incubated overnight at 4 ºC with primary antibodies diluted in Buffer A with 2.5 % BSA: mouse monoclonal anti-InlA (L7.7, 1:500 (Mengaud et al., 1996)); mouse monoclonal anti-InlB (D23.1, 1:2000 (Braun et al., 1999)); rabbit polyclonal

anti-Ami antiserum (R5, 1:5000 (Pascale Cossart, Institut Pasteur)); mouse monoclonal anti-ActA (abbexa, 1:1000) and rabbit polyclonal anti-*Lm* Glyceraldehyde-3-phosphate dehydrogenase (GAPDH) (Abgent, 1:5000). Membranes were washed three times with Buffer A and incubated during 1 h at room temperature with anti-mouse or anti-rabbit horseradish peroxidase (HRP)-conjugated secondary antibodies (P.A.R.I.S Biotech, 1:2000). Membranes were washed again and signals were detected using the Pierce® ECL Western Blotting Substrate (Thermo--Scientific) and digitally acquired in a ChemiDoc XRS+ system (Bio-Rad Laboratories). Signal intensity was quantified using Image J v1.5 f.

2.12. RNA sequencing

RNA extraction, mRNA enrichment, and poly(A) addition: Exponential-phase bacteria ($OD_{600\ nm}$~0.8) were centrifuged at 3800 g for 15 min at room temperature, and the bacterial pellet was washed with DMEM. Bacteria were then incubated in DMEM or DMEM supplemented with AMP (1 mM) for 1 h at 37 °C with 5 % CO_2. Total RNA was extracted by the phenol-chloroform extraction method, as previously described (Camejo et al., 2009), treated with TURBO DNA-free DNase I (Ambion), as recommended by the manufacturer, and checked for quality using a S2100 Bioanalyzer (Agilent Technologies). Ribosomal RNA was depleted via the MICROBExpress™ Bacterial mRNA Enrichment Kit (Thermo Fisher Scientific). Removal of rRNA was assessed using the S2100 BioAnalyser. Polyadenylation of non-polyadenylated transcripts was performed using 375 ng of ribodepleted mRNA, and *E. coli* poly(A) polymerase (New England Biolabs) for 1.5 min at 37 °C. Poly(A)+ RNA was purified using Agencourt RNAClean XP beads (Beckman Coulter).

Reverse transcription and preparation of full-length transcripts: Reverse transcription of polyadenylated mRNA and PCR amplification were performed according to the PCR-cDNA Barcoding protocol SQK-PCB111.24 (Oxford Nanopore Technologies). First-strand cDNA synthesis was carried out with 5 ng of poly(A)+ RNA, using supplied RT Primer (RTP), Strand Switching Primer II (SSPII), and Maxima H Minus Reverse Transcriptase (Thermo Fisher Scientific). Second-strand cDNA synthesis and PCR Barcoding were carried using a 15-cycle PCR reaction with supplied unique Barcode Primers, and LongAmp Hot Start Taq Master Mix (New England Biolabs). After amplification, samples were purified with AMPure XP beads (Beckman Coulter), washed with short-fragment buffer (SFB) and eluted in supplied Elution buffer. The cDNA products were treated with Exonuclease 1 (New England Biolabs) and purified using AMPure XP beads. Final cDNA concentrations were measured using the Qubit 1 × dsDNA High Sensitivity Assay (Invitrogen).

Library preparation and sequencing: Equimolar amounts of barcoded cDNA were multiplexed to prepare a sequencing library with 25 fmol of cDNA, used for ligation with the RAP T adapter and loaded on a R9.4.1 (FLO-MIN106) flow cell primed with the Flow Cell Priming Kit (EXP-FLP002). Sequencing was carried out for a maximum 72 h on a MinION 1 kb device with the MinKNOW software v23.11.7.

2.13. RNA sequencing data analysis

Basecalled FASTQ files were demultiplexed using Guppy barcoder (v6.1.5), and reads with low quality (Q score < 7) or barcode assignment failure were removed. Adapter and primer sequences were trimmed using Porechop (v0.2.4). Read quality was assessed using NanoPlot (v1.41.0). To assess differentially expressed genes between *L. monocytogenes* WT, Δ*purA* and Δ*purA*+AMP, clean sequencing reads were aligned to the reference genome sequence of *Listeria monocytogenes* EGD-e, using minimap2 (v2.24). Resulting SAM files were converted to sorted BAM format using SAMtools (v1.15). Gene-level read counts were obtained using featureCounts (Subread v2.0.3). Differential gene expression analysis was performed in EdgeR (v3.36.0) using a fixed biological coefficient of variation (BCV; BCV= 0.2). Analysis was performed using the "exact test" method and p-value adjusted using the false discovery rate (FDR) correction. Only genes with an adjusted p-value below 0.1 were considered.

2.14. Animal infections

Seven-week-old specific pathogen-free female BALB/c mice (Charles River Laboratories) were acclimatized for at least 7 days prior to infection and randomly assigned to four experimental groups (5–6 animals per cage/group). Mice were maintained at the i3S animal facilities, in high-efficiency particulate air (HEPA) filter-bearing cages under 12 h light cycles and in an *ad libitum* regimen of sterile chow and autoclaved water. For oral infection, 12 h starved animals were anaesthetized with isoflurane using a volatile anesthesia system and randomly inoculated by gavage with 10^9 CFUs of bacteria suspended in PBS with 150 mg/ml calcium carbonate ($CaCO_3$, Merck) to standardize stomach condition. Each group received a different strain: *L. monocytogenes* EGDe (positive control), Δ*purA*, +*purA* and Δ*purA* supplemented with AMP (1 mM). Sample sizes were guided by our 20 years of experience using similar analyses and researchers were aware of group allocation. Potential confounders such as treatment order, measurement order, or cage location were not controlled in this study. Welfare was assessed daily by measuring body weight and inspecting appearance (piloerection, posture), behavior, hydration, and respiration movement. Animals that succumbed to infection or required humane euthanasia prior to 72 h based on predefined endpoint criteria (e.g., >20 % body weight loss, markedly altered appearance, severely impaired behavior, signs of dehydration, or labored respiration) were excluded. Following these criteria, one animal from the +*purA* group was excluded from the analysis. At 72 h post-infection, animals were euthanized using a CO_2 inhalation system followed by cervical dislocation, and the liver, spleen and intestine were aseptically collected from each animal. The intestines were washed twice with EMEM, incubated in EMEM supplemented with 100 μg/ml gentamycin (Lonza) for 2 h, and washed twice in EMEM and once in PBS. Organs were homogenized in PBS, serially diluted, and plated on BHI agar plates (liver and spleen) or *Listeria* Selective Agar (Oxford formulation, OXOID) (intestine). The following day, CFUs of each strain were quantified. Animal procedures followed the guidelines of the European Commission for the handling of laboratory animals (Directive 2010/63/EU) and the Portuguese legislation for the use of animals for scientific purposes (Decreto-Lei 113/2013). All procedures were approved by the i3S Animal Ethics Committee and Direcção Geral de Alimentação e Veterinária (license 006564).

2.15. Statistical analysis

Statistical analysis was carried out with GraphPad Prism 10 software. Unpaired two-tailed Student's *t*-test was used to compare the means of two groups. One-way ANOVA with Dunnett's post-hoc test was used to compare the means relative to the mean of a control group, while Tukey's post-hoc test was used for pairwise comparison of means among more than two groups. Two-way ANOVA was used to analyse the interaction between two independent variables. For statistically significant differences, the following nomenclature has been used: * for $p < 0.05$; ** for $p < 0.01$; *** for $p < 0.001$; and **** for $p < 0.0001$.

3. Results

3.1. Validation of automated high-throughput microscopy screening

To identify new factors involved in the *L. monocytogenes* cell infection process, we conducted an automated high-throughput microscopy screening. For that, we constructed a *L. monocytogenes* EGDe strain constitutively expressing GFP from its chromosome (EGDe::pIMK-cGFP). We validated the screening approach by analysing a panel of mutants for genes previously established as critical for different stages of

the *L. monocytogenes* cell infection cycle. We included mutants for genes promoting cell internalization (*inlAB*) (Dramsi et al., 1995; Gaillard et al., 1991); rapid intracellular proliferation (*uhpT*) (Chico-Calero et al., 2002); or actin-based intracellular motility (*actA*) (Pillich et al., 2017). We confirmed that fluorescent WT, Δ*inlAB*, Δ*uhpT* and Δ*actA* strains grew similarly (Figure S1). The cell infection ability of these strains was tested by automated high-throughput microscopy. HeLa cells were infected (MOI 5) for 2 h, followed by a 15-hour gentamicin incubation. Automated fluorescence images (Fig. 1a) were analysed to quantify intracellular bacteria and total cells. While the number of total HeLa cells remained the same in all conditions, indicating no differences in cell survival, the number and the relative percentage of intracellular bacteria decreased for all the mutant strains (Δ*inlAB*, Δ*uhpT* and Δ*actA*) as compared to WT bacteria, thus reflecting the respective role of the deleted genes in cell infection (Fig. 1b-d). In parallel, HeLa cells were infected with *L. monocytogenes* WT and mutant strains in the same conditions (MOI 5 for 2 h, followed by a 15 h incubation with gentamicin), and intracellular bacteria were quantified by the conventional method (i.e. CFU numeration) (Fig. 1e,f). Results from conventional infection assays strongly corroborated those obtained by automated high-throughput microscopy, validating the method robustness and reliability.

3.2. Identification of *L. monocytogenes* transposon mutants impaired in cell infection

A library of 4224 *mariner*-based transposon insertion mutants was generated in *L. monocytogenes* EGDe serovar 1/2a, which provides a reasonable coverage of its 2.9 Mb genome (≈2900 genes) (Glaser et al., 2001). We implemented a machine learning model, developed and trained by imaging-derived features, to accurately screen the transposon-based mutant library and identify *L. monocytogenes* mutants with a defect in cell infection. High-throughput analysis revealed 231 transposon mutants with statistically significant (99 % of confidence) reduced levels of intracellular bacteria compared to *L. monocytogenes* WT. Decreased intracellular bacterial numbers suggested a defect in mutants' ability to enter, survive, or replicate within host cells. Transposon mutants with normalized bacteria-to-cell ratio values below the established threshold of 0.5 (relative to the WT strain) were classified as infection-deficient and selected for further analysis (Fig. 2a). The selected 231 candidate transposon mutants were re-tested under the same experimental conditions. 64 transposon mutants displayed statistically significant defects in cell infection compared to the WT strain (99 % of confidence, bacteria-to-cell ratio <0.6 as compared to WT) (Fig. 2b). The observed reduction in intracellular bacterial levels suggested that these mutants may be impaired in key virulence-related processes, such as host cell adhesion, invasion, intracellular replication, or cell-to-cell spread, and were therefore considered for further analysis.

The 64 statistically significant hits were re-tested using conventional infection assays (i.e. CFU numeration) under the same conditions (MOI 5 for 2 h, followed by 15 h incubation with gentamicin), to confirm their infectious capacity defect as compared to the WT or the invasion-defective Δ*inlAB* control strains. All the transposon mutants, excluding 1G5, 2A4, 8A2, 15E1, 21C7 and 33G11, showed a significantly decreased number of intracellular bacteria when compared with the WT strain (Fig. 3a).

3.3. High-throughput screening revealed new genes crucial for *L. monocytogenes* cell infection

Transposon insertion sites leading to decreased cell infection were identified by arbitrary PCR, sequencing and comparison with the *L. monocytogenes* EGDe genome (Glaser et al., 2001). From the 58 confirmed transposon mutants, we identified 24 different insertion loci corresponding to 14 genes spread over the *L. monocytogenes* EGDe genome (Fig. 3b,c). Fluorescence images representative of HeLa cells infected with the transposon mutants of the 14 different identified genes are shown in Figure S2. Five of these genes were previously involved in the *L. monocytogenes* cell infection process, including the adhesin Ami (Milohanic et al., 2000), the internalin InlA (Gaillard et al., 1991), the phagosomal membrane disrupting phospholipase PlcB (Marquis and Hager, 2000), the glutathione synthase GshF that controls the activity of major virulence factors (Reniere et al., 2015), and RmlB involved in wall teichoic acids glycosylation (Carvalho et al., 2015), thus validating our approach.

The nine remaining genes (*clpX, fur, lisK, prfB, proAB, purAB and lmo2217*) were selected for further characterization based on their potential new roles in *L. monocytogenes* cell infection. These genes encode the protease chaperone ClpX (Balogh et al., 2017), the ferric uptake regulator Fur (Ledala et al., 2007), the sensor histidine kinase LisK (Cotter et al., 2002), the peptide chain release factor 2 PrfB (Craigen and Caskey, 1986), proteins involved in the proline and purine biosynthesis (ProAB and PurAB, respectively) (Faith et al., 2012; Sleator et al., 2001), and Lmo2217 of unknown function. Genes were individually deleted from the *L. monocytogenes* EGDe chromosome, except *proA* and *proB* for which the entire *proAB* operon was removed. Despite numerous attempts, although the transposon mutants did not show any growth defects in BHI at 37 °C, we were unable to obtain *fur* and *prfB* deletion mutants. The growth profiles of the six constructed deletion mutants (Δ*proAB,* Δ*purA,* Δ*purB*, Δ*lisK,* Δ*clpX* and Δ*lmo2217*) were similar to that of the WT strain in nutrient-rich medium (Fig. 4a), indicating that bacterial growth in these conditions is independent from the deleted genes. Deletion mutants were then individually tested for their efficiency in infecting HeLa cells. Results confirmed that the six deletion mutants had a defect in the number of intracellular bacteria, as observed for the corresponding transposon mutants (Fig. 4b), corroborating automated high-throughput screening results and confirming the role of the deleted genes in *L. monocytogenes* cell infection.

3.4. Purine biosynthesis genes are essential for *L. monocytogenes* growth under nutrient-limiting conditions

Genes involved in purine biosynthesis (*purAB*) were overrepresented among the mutants displaying defective cell infection, with seven transposon mutants for *purA* and eight for *purB*, corresponding to five and three different insertion sites, respectively (Fig. 3b,c). This strongly suggested a particular role for these genes in the ability of *L. monocytogenes* to infect cultured cells. *purA* (*lmo0055*) encodes an adenylosuccinate synthetase that, together with the adenylosuccinate lyase PurB (Lmo1773) and other *pur* genes, is involved in purine biosynthesis. PurA catalyzes the conversion of inosine monophosphate (IMP) into adenylosuccinate, which is then converted by PurB into adenosine monophosphate (AMP), the precursor of adenosine and adenine (Benson and Gots, 1976).

We first confirmed the role of purine biosynthesis in *L. monocytogenes* EGDe growth. Whereas no significant differences were observed in a nutrient-rich medium (Fig. 5a), in minimal medium, the Δ*purA* strain exhibited a pronounced growth defect compared to the WT and the complemented strains (Fig. 5b), highlighting the importance of purine biosynthesis for bacterial growth under nutrient-limiting conditions. The growth defect of the Δ*purA* mutant was fully rescued by supplementing the medium with AMP or adenine (Fig. 5c,d), but not with ATP (Fig. 5e). Similar results were obtained with the Δ*purB* mutant (Figure S3). Scanning electron microscopy (SEM) analysis revealed that Δ*purA* bacteria grown in minimal medium exhibited an elongated cell morphology as compared to WT bacteria, a phenotype that was restored in the presence of AMP or adenine (Fig. 5f), suggesting that purine biosynthesis could play a role in cell wall homeostasis. We also confirmed the crucial role of PurA in intracellular multiplication into macrophages, as previously suggested (Feng et al., 2025; Fischer et al., 2022; Narayanan et al., 2022) (Figure S4).

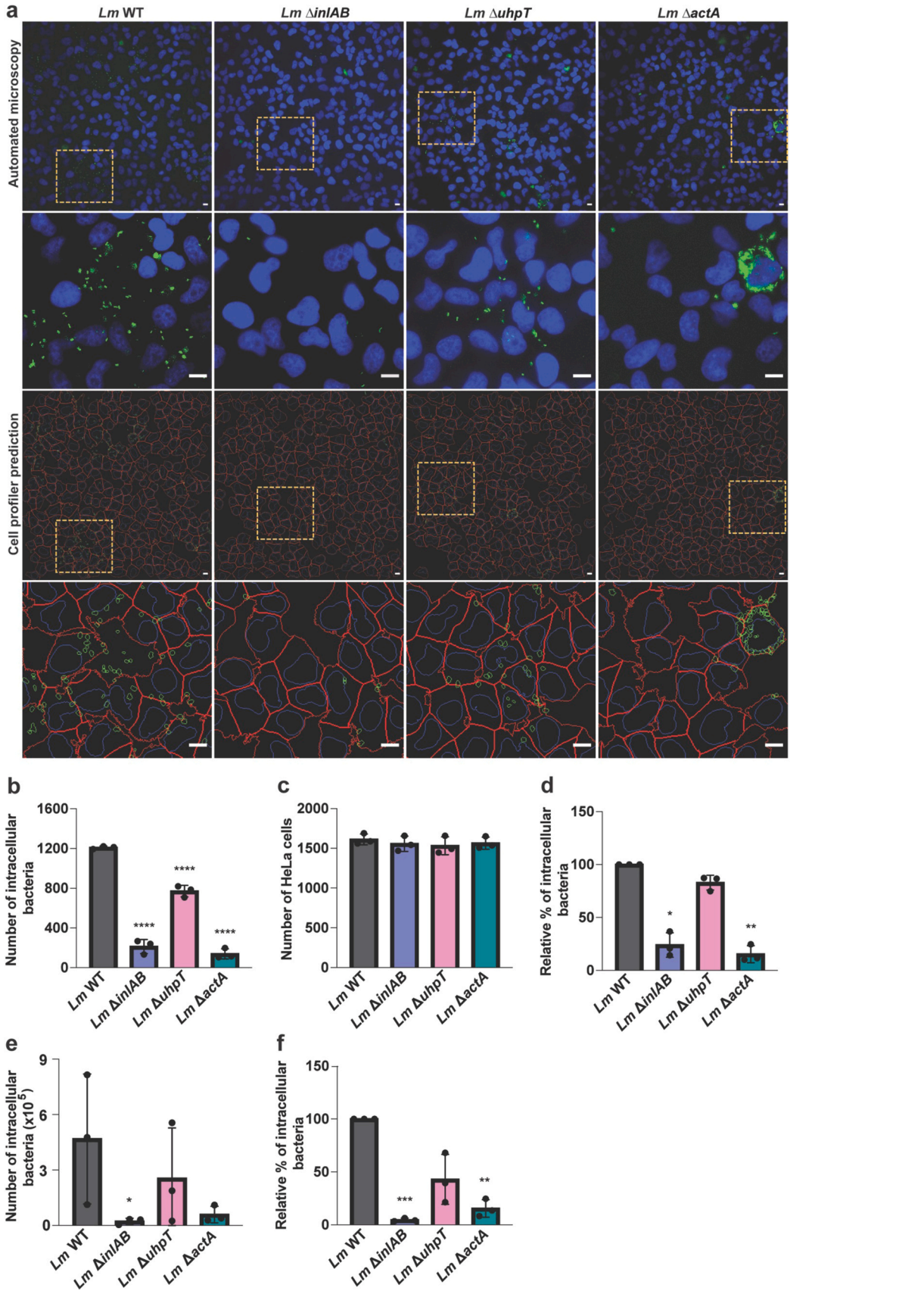

(caption on next page)

Fig. 1. High-throughput microscopy screen validation. (a) HeLa cells seeded in 96-well plates were infected with *L. monocytogenes* WT or the different mutant strains for 2 h and incubated for 15 h in the presence of gentamicin. Cells were washed, fixed and DNA was counterstained with DAPI. Representative images were acquired by automated microscopy. Nuclei in blue, bacteria in green and cell nuclei expansion in red. Scale bars, 10 μm. (b-d) Based on cell profiler predictions, the (b) number of intracellular bacteria and (c) total HeLa cells were automatically quantified for each acquired image, and (d) the relative percentage of intracellular bacteria normalized to *L. monocytogenes* WT values, arbitrarily fixed to 100 %, was calculated (e-f) Conventional invasion assays of HeLa cells infected by the different *L. monocytogenes* strains for 2 h plus 15 h in the presence of gentamicin. (e) Number of intracellular bacteria. (f) Relative % of intracellular bacteria shown as CFUs normalized to *L. monocytogenes* WT values, arbitrarily fixed to 100 %. Results are mean ± SD of three independent experiments. Differences from the *L. monocytogenes* WT *p < 0.05; **p < 0,01; ***p < 0,001; ****p < 0.0001.

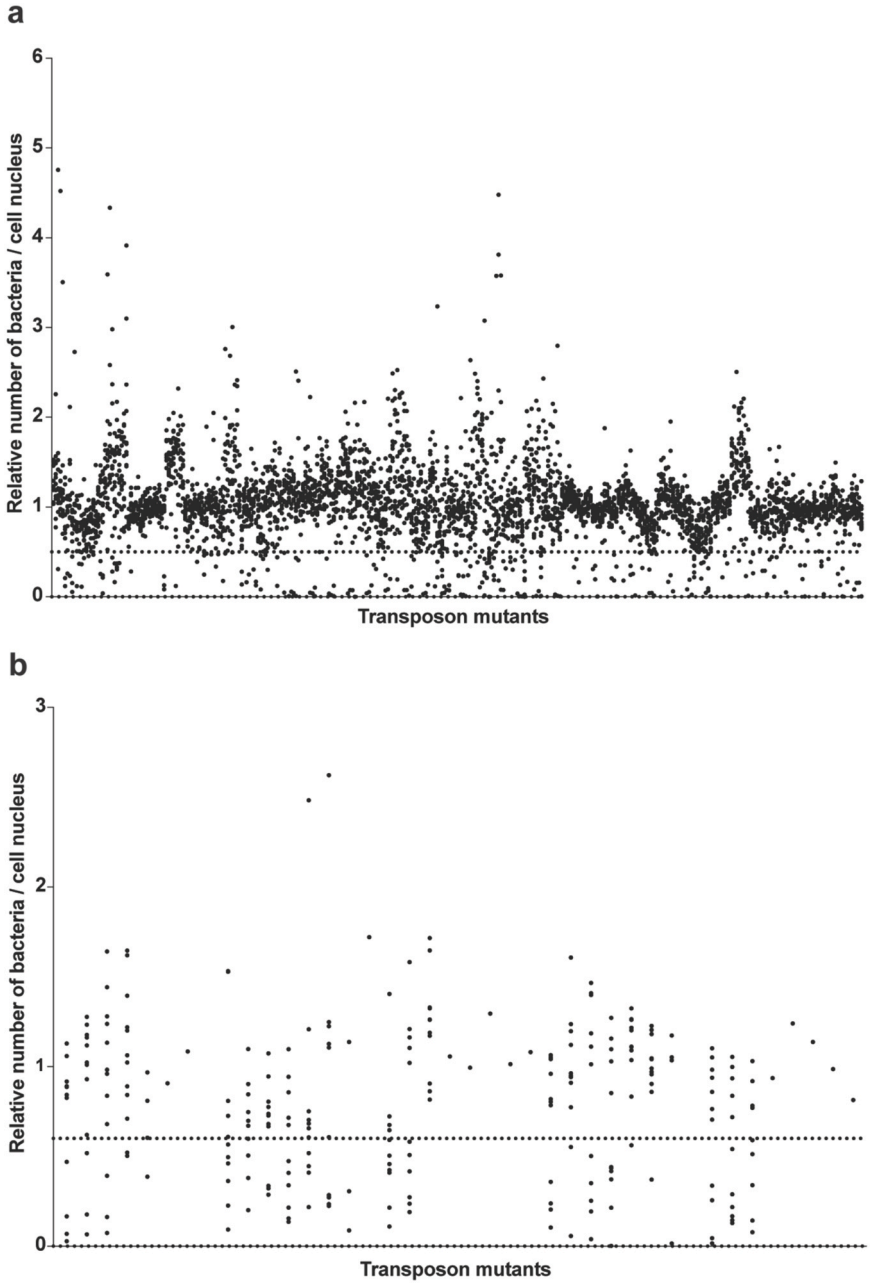

Fig. 2. Identification by automated high-throughput screening of *L. monocytogenes* transposon mutants impaired in cell infection. (a) HeLa cells were infected with a library composed by 4224 transposon mutants (MOI 5), for 2 h and incubated for 15 h in the presence of gentamicin, and analyzed by automated high-throughput microscopy. Each dot represents a transposon mutant. The ratio of the number of bacteria per cell for each transposon mutant was normalized to the levels of *L. monocytogenes* WT, plotted at 1. Mutants were identified as significant hits if their values fell below the WT average minus three times its standard deviation (99 % of confidence). The 231 mutants below the threshold (established at 0.5) were considered for further analysis. (b) HeLa cells were infected for 2 h and incubated for 15 h in the presence of gentamicin with the 231 transposon mutant candidates (MOI 5) and analyzed by automated high-throughput microscopy. Quantitative analysis revealed 64 statistically significant (99 % of confidence) transposon mutants below the threshold established at 0.6, normalized to the L. monocytogenes WT levels.

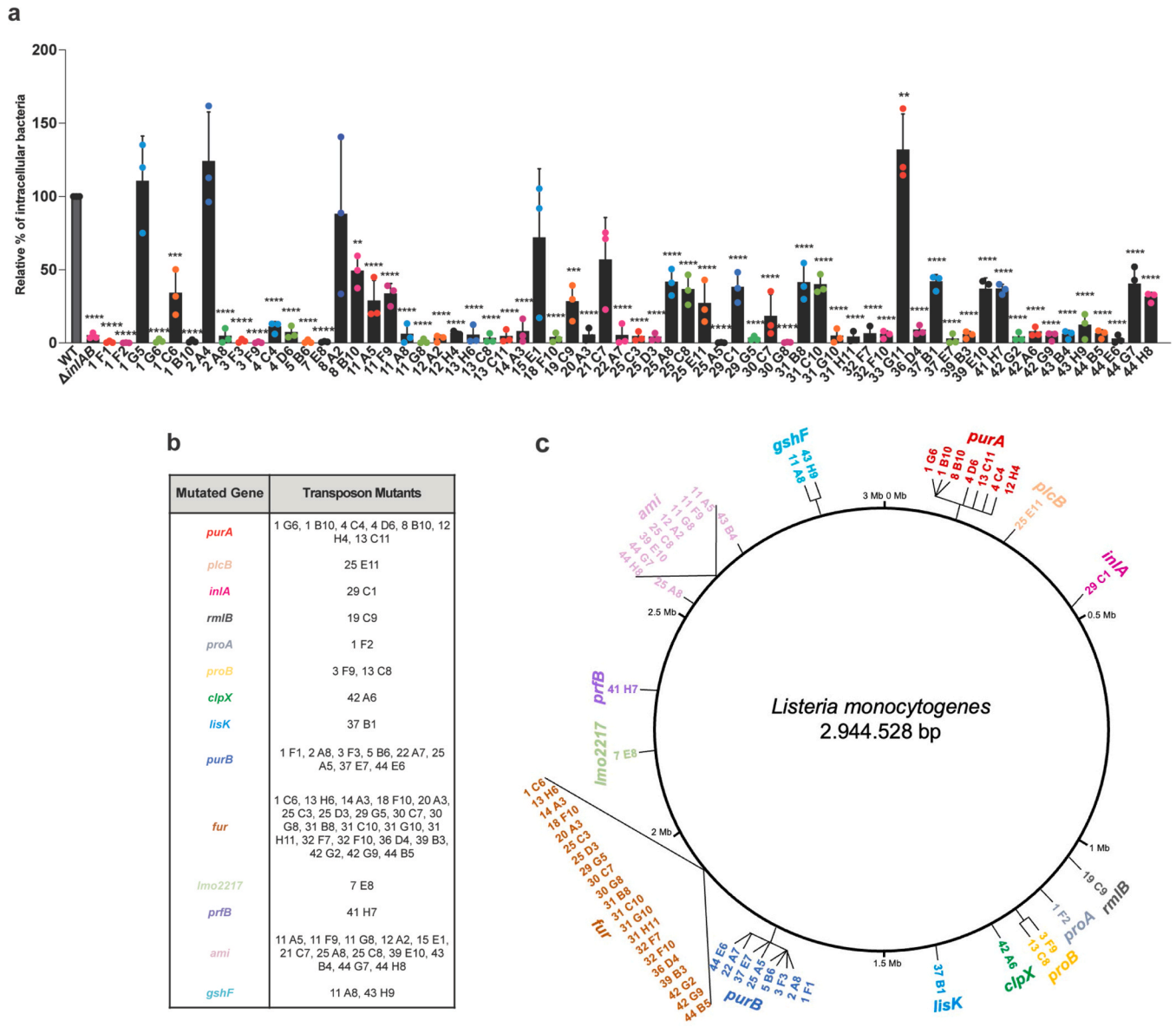

Fig. 3. High-throughput screen revealed fourteen genes crucial for *L. monocytogenes* cell infection. (a) HeLa cells were infected (MOI 5) with the 64 transposon mutants revealed by the high-throughput screen as having cell infection defects for 2 h and incubated for 15 h in the presence of gentamicin. Relative percentage of intracellular bacteria was shown as number of intracellular CFUs normalized to *L. monocytogenes* WT values arbitrarily fixed to 100. *L. monocytogenes* Δ*inlAB* was used as a non-invasive control. Results are mean ± SD of three independent experiments. Differences from the *L. monocytogenes* WT **p < 0.01; ***p < 0.001; ****p < 0.0001. (b) The 58 transposon mutants showing reduced percentage of intracellular bacteria as compared to the WT were sequenced to identify transposon insertion loci. For each transposon mutant is indicated the gene where the transposon is inserted. (c) Circular genome maps of *L. monocytogenes* EGDe showing the position of the 14 genes mutated and the corresponding 24 different insertion loci. The scale in megabases is indicated on the outside of the genome circles, with the origin of replication at position 0.

3.5. PurA is required for L. monocytogenes invasion of cultured cell lines

To analyze whether PurA could play an uncharacterized role in the early stages of cell infection, i.e. adhesion to or invasion of eukaryotic epithelial cells, we performed shorter infection assays (30 min or 1 h of infection plus 1.5 h of gentamicin treatment). Only a slight decrease was detected in the adherence of the Δ*purA* strain to HeLa cells (Figure S5). However, the Δ*purA* mutant was strongly impaired in cell invasion, showing significantly lower levels of intracellular bacteria as compared to the WT strain, in all the cell types tested (Fig. 6a-c). Supplementation with AMP at the time of the infection completely restored the invasion capacity of the Δ*purA* strain in HeLa cells, partially in Jeg-3 cells, and had no effect in CaCo-2 cells, pointing to a cell-specific purine-dependent entry mechanism (Fig. 6a-c). To definitively exclude a potential role of bacterial multiplication in the observed defect on intracellular bacteria numbers, we performed shorter infections of HeLa cells (45 min of infection plus 30 min of gentamicin). Results indicated that, even during a very short infection, the Δ*purA* mutant was strongly attenuated as compared to the WT and +*purA* strains (Fig. 6d), thus excluding any major contribution of bacterial intracellular multiplication and strongly suggesting that the absence of PurA affects *L. monocytogenes* internalization into cultured cells.

3.6. PurA-related cell invasion is independent from a direct effect of AMP on cultured cells

To assess if AMP treatment at the time of the infection could induce modifications of the host cells, in turn promoting unspecific

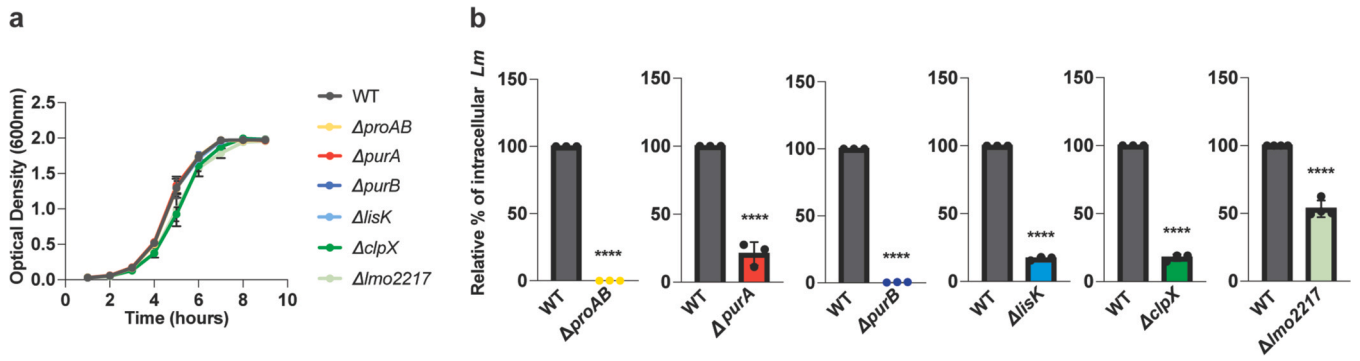

Fig. 4. Deletion mutants have a compromised intracellular behavior. (a) Growth curves of the different deletion mutant strains. Overnight cultures were diluted 100-fold in BHI medium and incubated at 37°C with agitation. Optical density was measured at 600 nm every hour during 9 h. (b) HeLa cells were infected (MOI 5) for 2 h and incubated for 15 h with gentamicin-containing medium, with the different *L. monocytogenes* deletion mutants, and relative percentage of intracellular bacteria was determined and shown as number of intracellular CFUs normalized to *L. monocytogenes* WT values, arbitrarily fixed to 100. Results are mean ± SD of three independent experiments. Differences from the *L. monocytogenes* WT *p < 0.05; ***p < 0.001; ****p < 0.0001.

internalization, we repeated invasion assays of HeLa cells using the non-invasive *L. innocua* strain in the presence or absence of AMP. Whereas AMP restored the invasion defect of the Δ*purA* strain, it did not promote *L. innocua* internalization (Fig. 7a) suggesting that AMP does not promote unspecific bacteria uptake. Interestingly, the addition of AMP at the time of the infection slightly increased the invasive capacity of the WT and +*purA* strains (Fig. 7a). To exclude any direct effect of AMP on cultured cells that would promote bacterial internalization, HeLa cells were pre-treated with AMP for one hour before being washed and infected with WT or the Δ*purA* strains in the absence or presence of AMP. Pre-incubation of cells with AMP had no effect on the internalization of WT and Δ*purA* bacteria (Fig. 7b). As observed in Fig. 7a, addition of AMP at the time of the infection restored Δ*purA* invasiveness to WT levels, an effect that is slightly accentuated by the pre-treatment of HeLa cells with AMP. We also controlled that, after the addition of AMP on HeLa cells, extracellular AMP levels remain constant over time (Fig. 7c), suggesting that host cells did not significantly uptake or metabolize AMP.

3.7. PurA is essential for in vivo L. monocytogenes virulence

We demonstrated the crucial role of *purA* in the virulence of *L. monocytogenes* EGDe 1/2a by orally infecting mice with the WT, Δ*purA* and +*purA* strains and assessing bacterial loads in the liver, spleen, and intestine 72 h post-infection. A significant reduction in the number of Δ*purA* bacteria was observed in all mouse organs as compared to the WT and +*purA* strains (Fig. 8a-c). As AMP was capable to restore the cell invasion capacity of the Δ*purA* strain *in vitro*, we assessed if supplementation with AMP during mouse oral infection was able to rescue bacterial virulence of the Δ*purA* mutant *in vivo*. Contrarily to what was observed during *in vitro* cell invasion assays, AMP supplementation of the bacteria inoculum at the time of infection had no effect on the virulence of the Δ*purA* mutant (Fig. 8a-c).

3.8. PurA supports GAPDH association with the bacterial surface

We hypothesized that purine metabolism could directly or indirectly regulate the expression of invasion-related genes (Goncheva et al., 2020). However, performing RNA sequencing experiments, we found only two genes differentially expressed in the Δ*purA* mutant as compared to the WT strain. The *lmo1884* gene, which encodes a putative purine permease potentially involved in purine export, was found to be downregulated in the absence of *purA*. In contrast, the glutathione synthase–encoding gene *gshF* appeared upregulated in the Δ*purA* mutant, possibly as a compensatory response to redox imbalance arising from defective purine metabolism (adjusted p-value = 0.02395 and 0.00647, respectively). We thus excluded a PurA-dependent regulation of virulence gene expression to explain the decreased invasiveness of the *purA* deletion mutant.

To determine if the impaired cell invasion capacity of the Δ*purA* mutant could be caused by an incorrect localization and/or abundance of major *L. monocytogenes* virulence factors in the bacterial cell wall, we analysed the surface content of InlA, InlB, ActA and Ami in the WT and Δ*purA* strains, as well as in the Δ*purA* mutant in the presence of AMP. Western blot analyses were performed using InlA, InlB, ActA and Ami antibodies on surface protein extracts retrieved from exponential bacterial cultures. No significant variations were observed in the levels of surface virulence factors between the WT and Δ*purA* strains, except for surface InlA protein levels that were slightly decreased in the *purA* mutant as compared to the WT strain. However, this decrease was not reverted by AMP treatment (Fig. 9a-d).

We commonly use the glyceraldehyde-3-phosphate dehydrogenase (GAPDH) as an internal loading control for western blots on *Listeria* extracts (Carvalho et al., 2018). When assessing the content in surface virulence factors of the Δ*purA* mutant, we consistently observed a strong diminution of surface GAPDH as compared to the WT strain (Fig. 9e). Interestingly, this decrease in GAPDH levels at the bacterial surface was fully reversed by AMP treatment (Fig. 9e).

Altogether, these results suggest that the absence of PurA induces a significant decrease in the levels of surface GAPDH and an important loss of the cell internalization capacity of *L. monocytogenes*.

4. Discussion

In this study, we generated a random Mariner transposon mutant library of *L. monocytogenes* EGDe serovar 1/2a and use it for the first time in an automated high-throughput screen, to identify new factors involved in bacterial infection of epithelial cells. We identified 58 transposon mutants impaired in their ability to infect cultured epithelial cells, corresponding to 24 different insertion loci in 14 distinct genes spread over the *L. monocytogenes* genome. Mariner transposons exhibit low site specificity, targeting only the TA dinucleotide sequence, which is abundant in *L. monocytogenes* (Glaser et al., 2001; Lampe et al., 1996). This should enhance the randomness and efficiency of the transposon. However, our analysis revealed that some loci are over represented. This was particularly the case for the *fur* and *ami* genes. Of the 21 transposon mutants found in the *fur* gene, all were inserted at the same unique site, while the 10 transposon mutants found in the *ami* gene were inserted at three different loci. Similarly, *purA* and *purB* genes were over-targeted with 7 and 8 mutants corresponding to 5 and 3 insertion loci, respectively. The presence of genomic hotspots for TA sites in the bacterial genome could explain the non-randomness of *Himar1* transposon

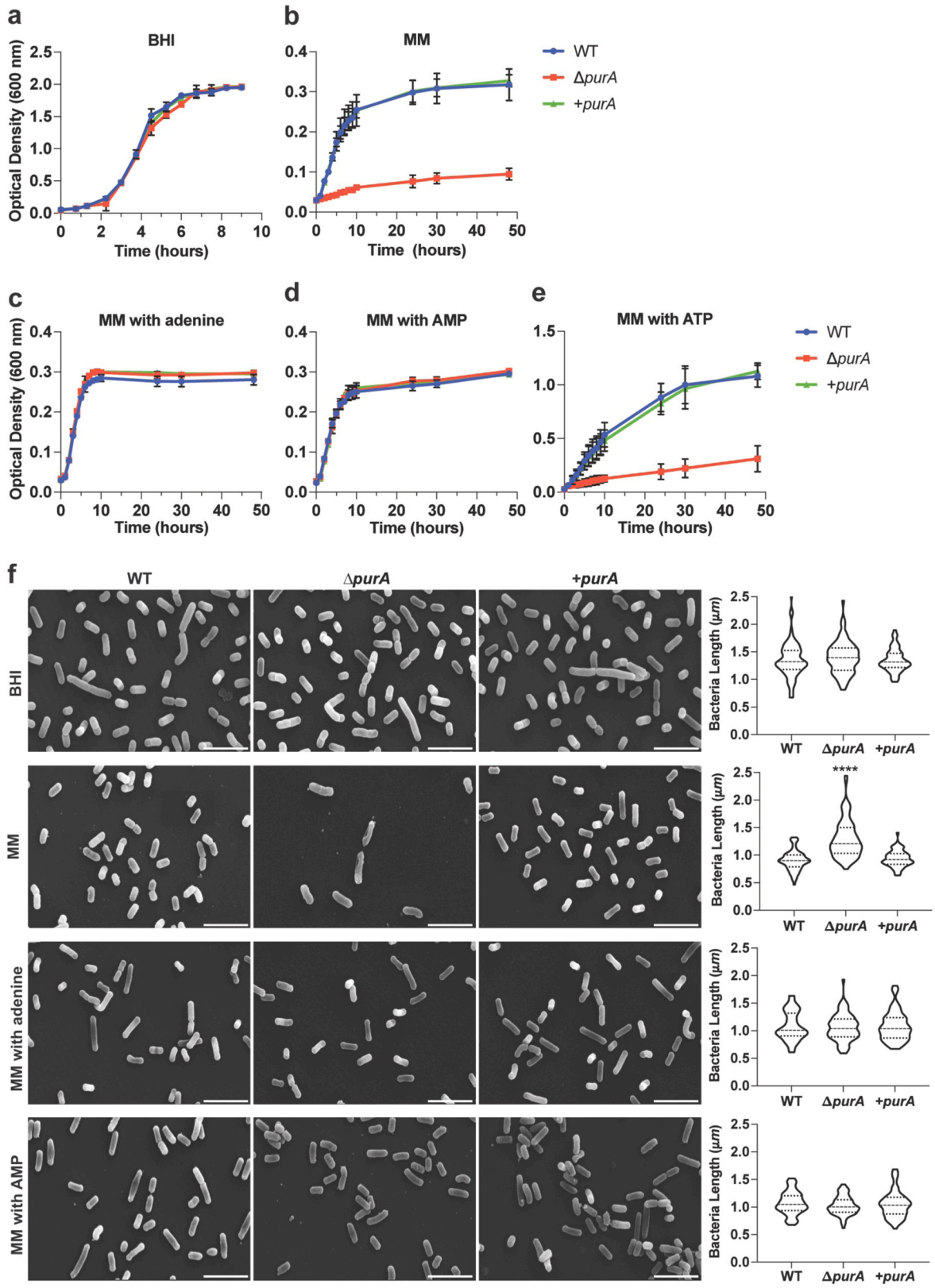

Fig. 5. PurA is essential for *L. monocytogenes* growth under nutrient-limiting conditions. Growth of *L. monocytogenes* WT, Δ*purA* mutant and the complemented strain (+*pur*A) in (a) rich Brain Heart Infusion medium (BHI), (b) minimal medium (MM), and MM supplemented with (c) adenine (1 mM), (d) AMP (1 mM) or (e) ATP (1 mM). Overnight cultures were diluted 100-fold, medium was supplemented or not, and incubated at 37.C with agitation. Optical density was measured at 600 nm (a) every 45 min during 9 h, (b-e) every hour during 10 h and twice a day for a maximum of 48 h. Results are mean ± SD of three independent experiments. Differences from *L. monocytogenes* WT *$p < 0.05$ (b) after 2 h of growth and (e) after 8 h of growth. (f) Scanning electron microscopy images of L. monocytogenes WT, Δ*purA* and +*purA* strains grown in BHI, MM and MM supplemented with adenine or AMP (1 mM) and the respective bacterial-length quantification. Images are representative from 3 independent assays. Scale bars 3 μm. Differences from *L. monocytogenes* WT ****$p < 0.0001$.

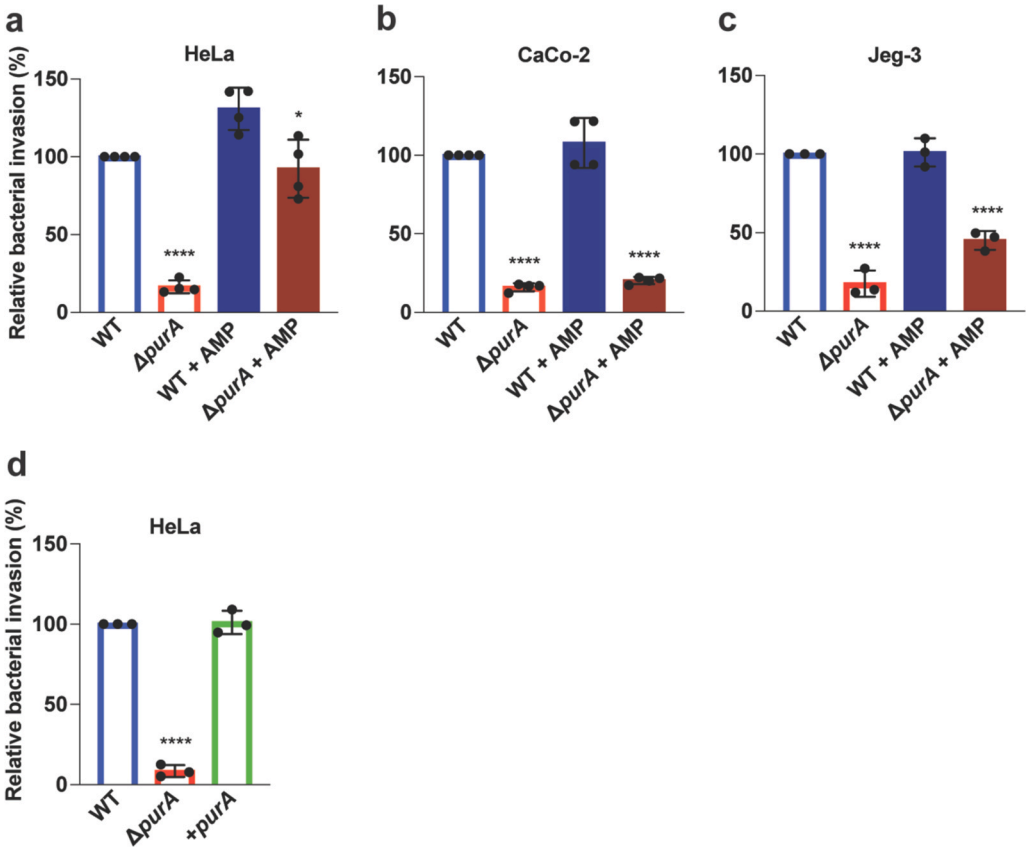

Fig. 6. PurA is required for *L. monocytogenes* invasion of cultured epithelial cell lines. Invasion of (a) HeLa, (b) Caco-2 and (c) Jeg-3 cells by *L. monocytogenes* WT and Δ*purA* strains, supplemented or not with AMP (1 mM) at the time of the infection. After 1 h of infection, cells were incubated for 1.5 h with gentamicin. Relative bacterial invasion is shown as number of CFUs normalized to *L. monocytogenes* WT values, arbitrarily fixed to 100. (d) Invasion of HeLa cells by *L. monocytogenes* WT, Δ*purA* and +*purA* strains for 45 min plus 30 min in the presence of gentamicin. Relative bacterial invasion is shown as number of CFUs normalized to *L. monocytogenes* WT values, arbitrarily fixed to 100. Results are mean ± SD of three independent experiments. Differences from *L. monocytogenes* WT ****$p < 0.0001$.

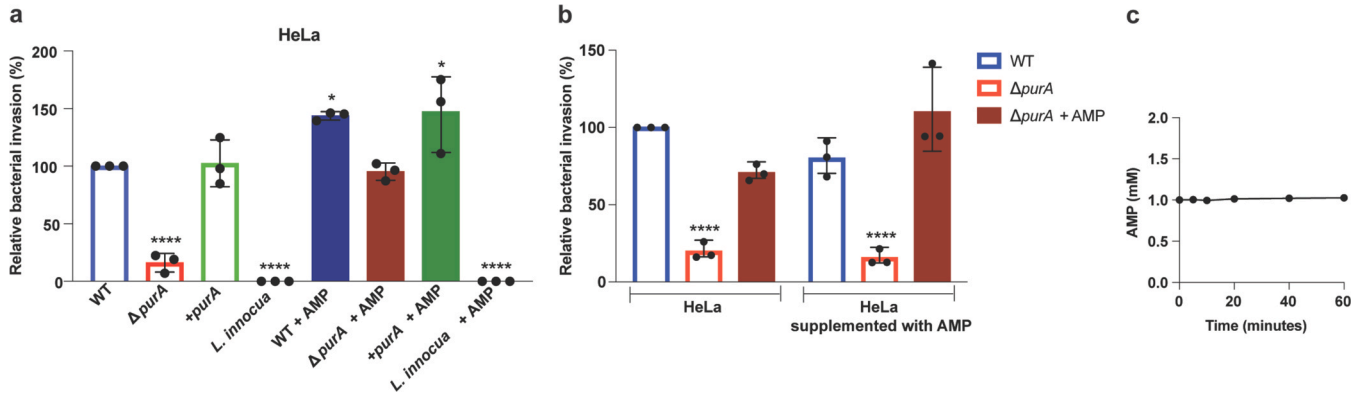

Fig. 7. PurA-related cell invasion is independent from a direct effect of AMP on cultured cells. (a) HeLa cells were infected with *L. monocytogenes* WT, Δ*purA*, +*purA* and *Listeria innocua*, supplemented or not with AMP (1 mM) at the time of the infection. After 1 h of infection, cells were incubated for 1.5 h with gentamicin. (b) Invasion of *L. monocytogenes* into HeLa cells supplemented or not with AMP (1 mM). After 1 h, HeLa cells were washed and infected with *L. monocytogenes* WT and Δ*purA* strains, supplemented or not with AMP (1 mM) at the time of the infection. After 1 h of infection, cells were incubated for 1.5 h with gentamicin. Bacterial invasion is shown as number of CFUs normalized to *L. monocytogenes* WT values arbitrarily fixed to 100. Results are mean ± SD of three independent experiments. Differences from *L. monocytogenes* WT ****$p < 0.0001$. (c) Upon the addition of 1 mM of AMP to the cells, extracellular levels of AMP were followed and quantified during 60 min by HPLC.

integration (Lampe et al., 1998; Lipkow et al., 2004). However, we were unable to locate any TA hotspots in the over-targeted regions of our screen. It was previously shown that experimental conditions used during the construction of the transposon library (42°C) can induce mutations affecting the activity of the alternative sigma factor B (SigB) because of the growth advantage conferred by these mutations under mild stress conditions (Guerreiro et al., 2020b). The observed disproportional rates of transposon insertions in certain genes could thus be due to their uncharacterized negative effects on SigB expression/activity.

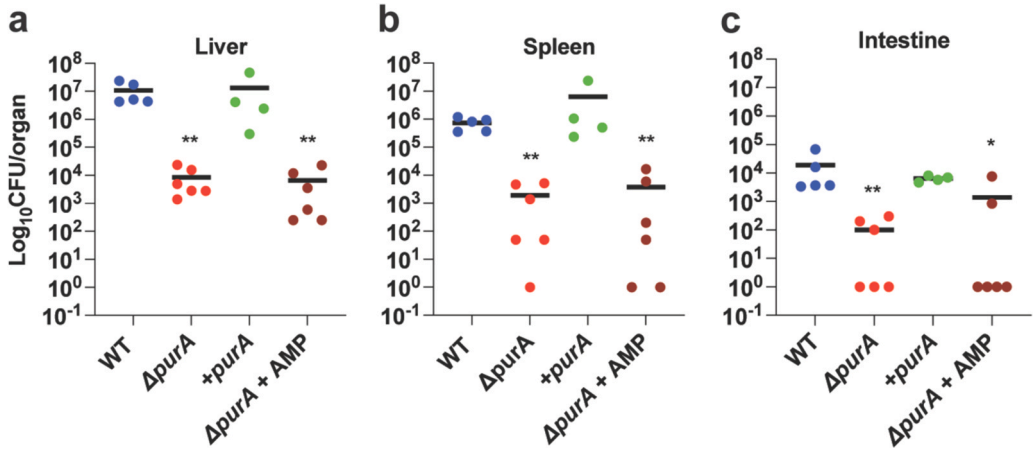

Fig. 8. PurA is essential for *in vivo L. monocytogenes* virulence. Bacterial counts of *L. monocytogenes* WT, Δ*purA* and +*purA* strains, and Δ*purA* supplemented with AMP strains in the liver, spleen and intestine of BALB/c mice 72 h after oral inoculation of 10^9 bacteria per animal. Data are presented as scatter plots, with each animal indicated by a dot and mean values indicated by a horizontal line (n = 5 or n = 6). Statistical analysis was performed individually between two groups with *t*-test. Differences from *L. monocytogenes* WT *p < 0.05; **p < 0.01.

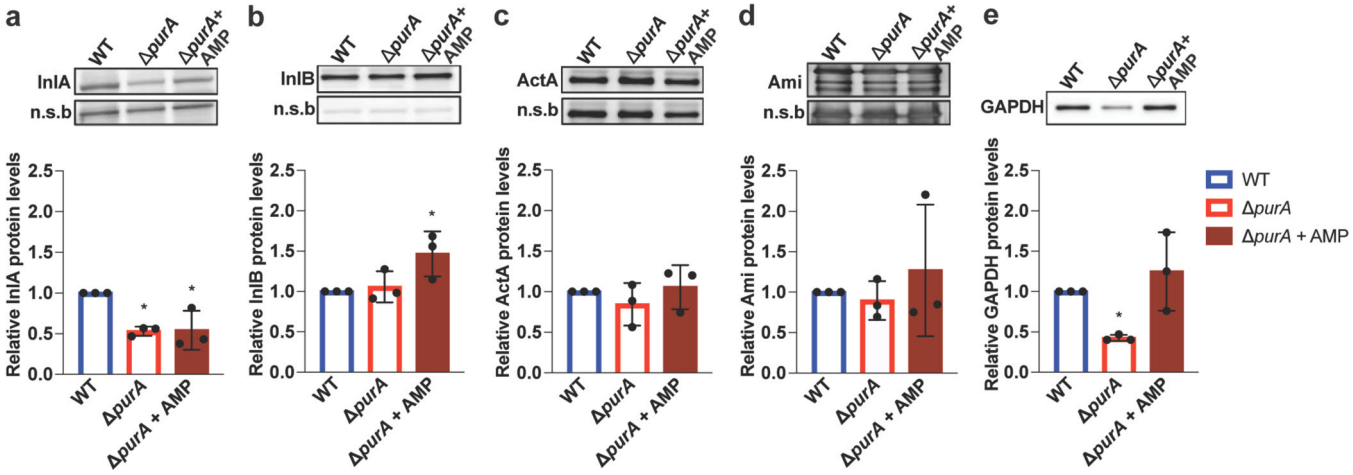

Fig. 9. PurA supports GAPDH association to bacterial surface. Western blot of *L. monocytogenes* surface protein extracts obtained from WT, Δ*purA* strains and Δ*purA* supplemented with AMP. The protein levels of a *L. monocytogenes* non-specific band (n.s.b) were used as sample loading control. Images are representative of three independent experiments and the band intensity of (a) InlA, (b) InlB, (c) ActA, (d) Ami and (e) GAPDH of the three assays was quantified and represented normalized to WT band intensity. Differences from *L. monocytogenes* WT *p < 0.05.

Among the 14 genes identified, five have previously been implicated in the *L. monocytogenes* cell infection process (*ami, inlA, plcB, gshF, rmlB*), validating our approach. In addition, automated high-throughput screening revealed 9 genes that were not previously involved in the aptitude of *L. monocytogenes* to infect cultured epithelial cells (*clpX, fur, lisK, prfB, proAB, purAB and lmo2217*).

ClpX is an ATP-dependent chaperone that recognizes protein substrates and directs unfolded peptide chains into the ClpP serine protease for degradation (Baker and Sauer, 2012; Balogh et al., 2022). The *L. monocytogenes* ClpXP complex mediates substrate recognition and degradation of proteins involved in transcriptional regulation and stress response (Balogh et al., 2022). A *clpX* mutant was shown to display defects in hemolytic activity and virulence (Zemansky et al., 2009). ClpX has been proposed to regulate the activity of LLO, the secreted pore-forming toxin essential for vacuole escape after *L. monocytogenes* internalization. This could explain the cell infection defect of the *clpX* mutant.

fur encodes a ferric uptake regulator involved in *Listeria* virulence, a behavior attributed to the deregulation of iron uptake and storage processes (Rea et al., 2004). Iron plays a crucial role in the ability of bacteria to enter and survive within cultured cells, being essential for bacterial growth, replication and various metabolic processes. Pathogenic bacteria often have mechanisms to acquire iron from their host environment. Whereas, to our knowledge, Fur was never directly implicated in cell invasion, iron availability was shown to affect *L. monocytogenes* entry into Caco-2 cells, with the enhanced invasive capability of iron-overloaded bacteria being correlated to higher expression of the *inlAB* genes (Conte et al., 1996).

lisK encodes the sensor histidine kinase of the LisRK two-component system involved in *L. monocytogenes* growth at low temperatures (Pöntinen et al., 2015), antimicrobial response (Cotter et al., 2002), osmotolerance (Sleator and Hill, 2005) and in virulence (Cotter et al., 1999). Following cell invasion, *L. monocytogenes* escapes from the vacuole and is released into the cell cytosol, where it senses and responds to various stresses and activates the production of virulence factors, many of them regulated by environmental conditions that could be sensed by the LisRK system (Cotter et al., 1999; Sleator and Hill, 2005).

prfB encodes a putative peptide chain release factor 2 that recognizes the UAA and UGA translational stop codons (Betney et al., 2010). It was previously identified in a mariner transposon-based signature-tagged mutagenesis screen as required for *L. monocytogenes* virulence in mice (Cummins et al., 2013). Its important role for terminating translation of

many proteins could explain our difficulty in obtaining a *prfB* deletion mutant.

The *proAB* operon encodes enzymes that catalyze the initial steps of proline biosynthesis. While proline is required for *L. monocytogenes* survival under high-pressure or high-osmolarity stress (Considine et al., 2011; Sleator et al., 2001), proline auxotrophy has no apparent impact on virulence (Sleator et al., 2001).

lmo2217 encodes a small protein of unknown function that seems to be regulated by the stress-response sigma factor SigB (Oliver et al., 2010). A transposon mutant for *lmo2217* was shown to have a hemolytic defect (Zemansky et al., 2009), which could indicate a reduction in the level or activity of LLO, that, in turn, may explain the cell infection defect we observed.

Among the genes identified here, we selected *purAB* for further study due to their over-representation among the transposon mutants showing a decreased cell infection phenotype. PurAB catalyze the conversion of IMP into AMP, and purine biosynthesis has been involved in the pathogenesis of several bacteria, including *Bacillus anthracis* (Ivánovics et al., 1968), *Yersinia pestis* (Brubaker, 1970), *Salmonella enterica* (McFarland and Stocker, 1987), *Streptococcus pneumoniae* (Liu et al., 2021; Polissi et al., 1998), *Streptococcus pyogenes* (Breton et al., 2013), *Edwardsiella piscicida* (Hu et al., 2022) and *Staphylococcus aureus* (Goncheva et al., 2020; Lan et al., 2010). *Escherichia coli* PurA has also been shown to be required for invasion of human brain microvascular endothelial cells and colonization *in vivo* (Hoffman et al., 2001; Ma et al., 2018; Sun et al., 2011). Previous studies have demonstrated that *L. monocytogenes purA* mutants are defective in replication within Caco-2 cells, macrophages or human serum, and in their ability to cause systemic infection in mice (Faith et al., 2012; Feng et al., 2025; Fischer et al., 2022; Narayanan et al., 2022). These phenotypes are thought to result from insufficient intracellular purine availability, creating a need for a functional bacterial biosynthetic apparatus.

Here, we confirmed the crucial role of *purA* in *L. monocytogenes* EGDe serovar 1/2a growth under nutrient-limiting conditions, intracellular survival and *in vivo* virulence, and further revealed its unexpected function in bacterial entry into eukaryotic epithelial cells. The cell internalization defect of the *purA* deletion mutant was rescued by AMP supplementation, pointing to a purine-dependent entry mechanism. This novel *purA*-dependent entry mechanism is independent of any direct effect of AMP on cultured cells, as AMP treatment did not promote bacterial uptake. Moreover, HeLa cells showed minimal AMP uptake, supporting the notion that AMP must be directly available to the bacteria, rather than relying on host-mediated effects. While AMP restored the invasion capacity of the *purA* mutant in HeLa cells, it only partially reestablished bacterial entry into Jeg-3 cells, and had no effect in CaCo-2 cells. HeLa cells are non-polarized, loosely adherent, and lack intercellular junctions, allowing direct contact between bacteria, the extracellular medium (containing AMP), and the host membrane. In contrast, Caco-2 cells, even under our culture conditions, are slightly polarized and possess tight junctions that may restrict bacterial and AMP diffusion. Jeg-3 cells display an intermediate phenotype, with partial polarization capacity and some junctional organization. The access of bacteria to AMP may thus mainly depend on the host cell surface architecture, which differs among the cell types used. *L. monocytogenes* enters cell types through distinct pathways: via the InlB–c-Met route in HeLa cells, the InlA–E-cadherin route in Caco-2 cells, and through both routes in Jeg-3 cells (Pizarro-Cerdá et al., 2012). The requirement for or role of AMP may therefore also differ depending on the entry pathway utilized.

The absence of PurA does not significantly interfere with gene expression, and regarding major surface virulence factors, only InlA levels were reduced. However, HeLa cells do not express E-cadherin (Vessey et al., 1995), the specific cell receptor for InlA, and thus *L. monocytogenes* invasion of HeLa cells is InlA-independent (Auriemma et al., 2010; Pizarro-Cerdá et al., 2012). This suggests that the Δ*purA* defect in cell invasion is most probably unrelated to decreased levels of surface-exposed InlA. Unexpectedly, we observed a marked and consistent diminution of surface-localized GAPDH in the *purA* deletion mutant, which was reverted by AMP addition. GAPDH is a glycolytic enzyme catalyzing the conversion of glyceraldehyde-3-phosphate to 1, 3-bisphosphoglycerate (Winterbourn et al., 2023), but additional roles unrelated to its enzymatic function have been demonstrated. *L. monocytogenes* GAPDH was previously shown to bind to the host Rab5a GTPase at the phagosomal membrane, delaying phagosome-endosome fusion and allowing bacteria to escape lysosomal degradation and survive within host cells (Alvarez-Dominguez et al., 2008). The presence of surface-exposed GAPDH was described in several bacterial species, being primarily attributed to cell lysis mediated by bacterial autolysins (Kopeckova et al., 2020). We hypothesize that the absence of PurA could induce changes in bacterial surface properties that would stabilize the cell wall to avoid autolysis under stress in turn reducing cytosolic GAPDH release, or would destabilize the cell wall in turn reducing surface GAPDH retention. In many pathogenic bacteria, surface-localized GAPDH binds to components related to the extracellular matrix (ECM), plasminogen being the most common target (Kopeckova et al., 2020). Surface-bound plasminogen is then activated by plasminogen activators into proteolytic plasmin, which degrades ECM proteins, promoting bacterial cell invasion (Bhattacharya et al., 2012; Peetermans et al., 2016), a process known as bacterial metastasis (Lähteenmäki et al., 2005). This is the particular case of *Mycobacterium tuberculosis* GAPDH that binds plasminogen at the bacterial surface to promote invasion of lung epithelial cells (Gani et al., 2021). We can thus postulate that in a *purA* mutant, the purine metabolism is altered, possibly being a signal for a stress response that would alter GAPDH surface localization, in turn potentially impacting plasminogen binding and reducing bacterial invasiveness.

5. Conclusion

To uncover novel genetic factors required for *L. monocytogenes* cell infection, we developed an automated high-throughput microscopy screening pipeline. Using this approach, we screened a *L. monocytogenes* transposon mutant library and identified new bacterial genes implicated in cell infection, inclusing genes encoding the protease chaperone ClpX, the ferric uptake regulator Fur, the sensor histidine kinase LisK, the peptide chain release factor 2 PrfB, proteins involved in proline and purine biosynthesis (ProAB, PurAB), and Lmo2217, a protein of unknown function. The targeted deletion of the PurA encoding gene revealed an unexpected role for this adenylosuccinate synthetase in maintaining surface localization of the putative plasminogen-binding protein GAPDH and promoting bacterial entry into host cells. Overall, these findings highlight the power of automated high-throughput microscopy screening to dissect host–pathogen interactions and advance our understanding of *L. monocytogenes* intracellular pathogenesis.

Funding

This work was supported by National Funds through FCT - Fundação para a Ciência e a Tecnologia, I.P, under projects UIDB/04293/2020 (D. Cabanes) and UID/50016/2025 (B.G. Bernardes), and by ESCMID Research Grant (R. Pombinho). Rita Pombinho and Sandra Sousa received support from the FCT CEEC program (2021.02924.CEECIND and 2022.04457.CEECIND respectively). Ângela Sofia Alves, Diana Meireles, and Beatriz G. Bernardes received FCT PhD fellowships (2020.08891.BD, 2021.04806.BD, and 2021.05717.BD respectively).

CRediT authorship contribution statement

Diana Meireles: Writing – review & editing, Investigation. **Chiara Suriano:** Investigation. **Alves Angela:** Writing – review & editing, Writing – original draft, Visualization, Validation, Methodology, Investigation, Formal analysis, Data curation, Conceptualization. **Bernardes**

Beatriz G: Investigation. **Sandra Sousa:** Writing – review & editing, Writing – original draft, Investigation, Formal analysis, Conceptualization. **Ricardo Monteiro:** Writing – review & editing, Investigation. **Rute Oliveira:** Writing – review & editing, Investigation. **Rita Pombinho:** Writing – review & editing, Writing – original draft, Supervision, Investigation, Data curation, Conceptualization. **Didier Cabanes:** Writing – review & editing, Writing – original draft, Validation, Supervision, Resources, Project administration, Methodology, Funding acquisition, Formal analysis, Data curation, Conceptualization.

Declaration of Competing Interest

The authors report there are no competing interests to declare.

Acknowledgments

The authors acknowledge the support of the i3S Scientific Platforms - BioSciences Screening, Biochemical and Biophysical Technologies, and Bioinformatics.

Appendix A. Supporting information

Supplementary data associated with this article can be found in the online version at doi:10.1016/j.micres.2026.128442.

Data availability

Data will be made available on request.

References

Agaisse, H., Burrack, L.S., Philips, J.A., Rubin, E.J., Perrimon, N., Higgins, D.E., 2005. Genome-wide RNAi screen for host factors required for intracellular bacterial infection. Science 309, 1248–1251. https://doi.org/10.1126/SCIENCE.1116008.

Alvarez-Dominguez, C., Madrazo-Toca, F., Fernandez-Prieto, L., Vandekerckhove, J., Pareja, E., Tobes, R., Gomez-Lopez, M.T., Del Cerro-Vadillo, E., Fresno, M., Leyva-Cobián, F., Carrasco-Marín, E., 2008. Characterization of a *Listeria monocytogenes* protein interfering with Rab5a. Traffic 9, 325–337. https://doi.org/10.1111/j.1600-0854.2007.00683.x.

Arnaud, M., Chastanet, A., Débarbouillé, M., 2004. New vector for efficient allelic replacement in naturally nontransformable, low-GC-content, gram-positive bacteria. Appl. Environ. Microbiol 70, 6887. https://doi.org/10.1128/AEM.70.11.6887-6891.2004.

Auriemma, C., Viscardi, M., Tafuri, S., Pavone, L.M., Capuano, F., Rinaldi, L., Della Morte, R., Iovane, G., Staiano, N., 2010. Integrin receptors play a role in the internalin B-dependent entry of *Listeria monocytogenes* into host cells. Cell Mol. Biol. Lett. 15, 496–506. https://doi.org/10.2478/S11658-010-0019-Z.

Baker, T.A., Sauer, R.T., 2012. ClpXP, an ATP-powered unfolding and protein-degradation machine. Biochim. Biophys. Acta (BBA) Mol. Cell Res. 1823, 15–28. https://doi.org/10.1016/J.BBAMCR.2011.06.007.

Balestrino, D., Anne Hamon, M., Dortet, L., Nahori, M.A., Pizarro-Cerda, J., Alignani, D., Dussurget, O., Cossart, P., Toledo-Arana, A., 2010. Single-cell techniques using chromosomally tagged fluorescent bacteria to study *Listeria monocytogenes* infection processes. Appl. Environ. Microbiol. 76, 3625–3636. https://doi.org/10.1128/AEM.02612-09.

Balogh, D., Dahmen, M., Stahl, M., Poreba, M., Gersch, M., Drag, M., Sieber, S.A., 2017. Insights into ClpXP proteolysis: heterooligomerization and partial deactivation enhance chaperone affinity and substrate turnover in *Listeria monocytogenes*. Chem. Sci. 8, 1592–1600. https://doi.org/10.1039/C6SC03438A.

Balogh, D., Eckel, K., Fetzer, C., Sieber, S.A., 2022. *Listeria monocytogenes* utilizes the ClpP1/2 proteolytic machinery for fine-tuned substrate degradation at elevated temperatures. RSC Chem. Biol. 3, 955–971. https://doi.org/10.1039/D2CB00077F.

Benson, C.E., Gots, J.S., 1976. Occurrence of a regulatory deficiency in purine biosynthesis among purA mutants of *Salmonella typhimurium*. MGG Mol. Gen. Genet. 145, 31–36. https://doi.org/10.1007/BF00331554.

Betney, R., De Silva, E., Krishnan, J., Stansfield, I., 2010. Autoregulatory systems controlling translation factor expression: thermostat-like control of translational accuracy. RNA 16, 655–663. https://doi.org/10.1261/RNA.1796210.

Bhattacharya, S., Ploplis, V.A., Castellino, F.J., 2012. Bacterial plasminogen receptors utilize host plasminogen system for effective invasion and dissemination. Biomed. Res. Int. 2012, 482096. https://doi.org/10.1155/2012/482096.

Braun, L., Nato, F., Payrastre, B., Mazié, J.C., Cossart, P., 1999. The 213-amino-acid leucine-rich repeat region of the *Listeria monocytogenes* InlB protein is sufficient for entry into mammalian cells, stimulation of PI 3-kinase and membrane ruffling. Mol. Microbiol. 34, 10–23. https://doi.org/10.1046/J.1365-2958.1999.01560.X.

Breton, Y.Le, Mistry, P., Valdes, K.M., Quigley, J., Kumar, N., Tettelin, H., McIvera, K.S., 2013. Genome-wide identification of genes required for fitness of group a streptococcus in human blood. Infect. Immun. 81, 862–875. https://doi.org/10.1128/IAI.00837-12.

Brubaker, R.R., 1970. Interconversion of purine mononucleotides in *Pasteurella pestis*. Infect. Immun. 1, 446–454. https://doi.org/10.1128/IAI.1.5.446-454.1970.

Camejo, A., Buchrieser, C., Couvé, E., Carvalho, F., Reis, O., Ferreira, P., Sousa, S., Cossart, P., Cabanes, D., 2009. In vivo transcriptional profiling of *Listeria monocytogenes* and mutagenesis identify new virulence factors involved in infection. PLoS Pathog. 5, e1000449. https://doi.org/10.1371/JOURNAL.PPAT.1000449.

Carvalho, F., Atilano, M.L., Pombinho, R., Covas, G., Gallo, R.L., Filipe, S.R., Sousa, S., Cabanes, D., 2015. L-Rhamnosylation of *Listeria monocytogenes* wall teichoic acids promotes resistance to antimicrobial peptides by delaying interaction with the membrane. PLOS Pathog. 11, e1004919. https://doi.org/10.1371/JOURNAL.PPAT.1004919.

Carvalho, F., Sousa, S., Cabanes, D., 2018. l-Rhamnosylation of wall teichoic acids promotes efficient surface association of *Listeria monocytogenes* virulence factors InlB and Ami through interaction with GW domains. Environ. Microbiol. 20, 3941–3951. https://doi.org/10.1111/1462-2920.14351.

Chico-Calero, I., Suárez, M., González-Zorn, B., Scortti, M., Slaghuis, J., Werner, Goebel, Glaser, P., Amend, A., Baquero, F., Berche, P., Bloecker, H., Brandt, P., Buchrieser, C., Chakraborty, T., Charbit, A., Couvé, E., De Daruvar, A., Dehoux, P., Domann, E., Domínguez-Bernal, G., Durand, L., Entian, K.D., Frangeul, L., Fsihi, H., Del Portillo, F.G., Garrrido, P., Goebel, W., Gómez-López, N., Hain, T., Hauf, J., Jackson, D., Kreft, J., Kunst, F., Mata-Vicente, J., Ng, E., Nordsiek, G., Pérez-Díaz, J. C., Remmel, B., Rose, M., Rusniok, C., Schluetter, T., Tierrez, A., Vázquez-Boland, J. A., Voss, H., Wehland, J., Cossart, P., 2002. Hpt, a bacterial homolog of the microsomal glucose-6-phosphate translocase, mediates rapid intracellular proliferation in *Listeria*. Proc. Natl. Acad. Sci. USA 99, 431–436. https://doi.org/10.1073/PNAS.012363899.

Considine, K.M., Sleator, R.D., Kelly, A.L., Fitzgerald, G.F., Hill, C., 2011. A role for proline synthesis and transport in *Listeria monocytogenes* barotolerance. J. Appl. Microbiol. 110, 1187–1194. https://doi.org/10.1111/J.1365-2672.2011.04982.X.

Conte, M.P., Longhi, C., Polidoro, M., Petrone, G., Buonfiglio, V., Santo, S.D.I., Papi, E., Seganti, L., Visca, P., Valenti, P., 1996. Iron availability affects entry of *Listeria monocytogenes* into the enterocytelike cell line Caco-2. Infect. Immun. 64, 3925–3929. https://doi.org/10.1128/IAI.64.9.3925-3929.1996.

Cossart, P., 2011. Illuminating the landscape of host-pathogen interactions with the bacterium *Listeria monocytogenes*. Proc. Natl. Acad. Sci. USA 108, 19484–19491. https://doi.org/10.1073/PNAS.1112371108.

Cotter, P.D., Emerson, N., Gahan, C.G.M., Hill, C., 1999. Identification and disruption of lisRK, a genetic locus encoding a two-component signal transduction system involved in stress tolerance and virulence in *Listeria monocytogenes*. J. Bacteriol. 181, 6840–6843. https://doi.org/10.1128/JB.181.21.6840-6843.1999.

Cotter, P.D., Guinane, C.M., Hill, C., 2002. The LisRK signal transduction system determines the sensitivity of *Listeria monocytogenes* to nisin and cephalosporins. Antimicrob. Agents Chemother. 46, 2784–2790. https://doi.org/10.1128/AAC.46.9.2784-2790.2002.

Craigen, W.J., Caskey, C.T., 1986. Expression of peptide chain release factor 2 requires high-efficiency frameshift, 1986 322:6076 Nature 322, 273–275. https://doi.org/10.1038/322273a0.

Cummins, J., Casey, P.G., Joyce, S.A., Gahan, C.G.M., 2013. A mariner transposon-based signature-tagged mutagenesis system for the analysis of oral infection by *Listeria monocytogenes*. PLoS One 8, e75437. https://doi.org/10.1371/JOURNAL.PONE.0075437.

Dramsi, S., Biswas, I., Maguin, E., Braun, L., Mastroeni, P., Cossart, P., 1995. Entry of *Listeria monocytogenes* into hepatocytes requires expression of InlB, a surface protein of the internalin multigene family. Mol. Microbiol. 16, 251–261. https://doi.org/10.1111/J.1365-2958.1995.TB02297.X.

Faith, N.G., Kim, J.W., Azizoglu, R., Kathariou, S., Czuprynski, C., 2012. Purine biosynthesis mutants (purA and purB) of serotype 4b *Listeria monocytogenes* are severely attenuated for systemic infection in intragastrically inoculated A/j mice. ⟨https://home.liebertpub.com/fpd⟩ 9, 480–486. https://doi.org/10.1089/FPD.2011.1013.

Feng, Y., Lobanovska, M., Vickery, J., Castillo, J.G., Güereca, L., Chang, S.K., DuPage, M., Portnoy, D.A., 2025. *Listeria monocytogenes* adenosine auxotrophs are impaired for intracellular and extracellular growth but retain potent immunogenicity. Infect. Immun. https://doi.org/10.1128/IAI.00343-25.

Fischer, M.A., Engelgeh, T., Rothe, P., Fuchs, S., Thürmer, A., Halbedel, S., 2022. *Listeria monocytogenes* genes supporting growth under standard laboratory cultivation conditions and during macrophage infection. Genome Res. 32, 1711–1726. https://doi.org/10.1101/GR.276747.122.

Food Safety Authority, E., Centre for Disease Prevention, E., 2024. The European union one health 2023 zoonoses report. EFSA J. 22, e9106. https://doi.org/10.2903/J.EFSA.2024.9106.

Gaillard, J.L., Berche, P., Frehel, C., Gouln, E., Cossart, P., 1991. Entry of *L. monocytogenes* into cells is mediated by internalin, a repeat protein reminiscent of surface antigens from gram-positive cocci. Cell 65, 1127–1141. https://doi.org/10.1016/0092-8674(91)90009-N.

Gani, Z., Boradia, V.M., Kumar, A., Patidar, A., Talukdar, S., Choudhary, E., Singh, R., Agarwal, N., Raje, M., Iyengar Raje, C., 2021. *Mycobacterium tuberculosis* glyceraldehyde-3-phosphate dehydrogenase plays a dual role—as an adhesin and as a receptor for plasmin(ogen). Cell Microbiol. 23, e13311. https://doi.org/10.1111/CMI.13311.

Glaser, P., Frangeul, L., Buchrieser, C., Rusniok, C., Amend, A., Baquero, F., Berche, P., Bloecker, H., Brandt, P., Chakraborty, T., Charbit, A., Chetouani, F., Couvé, E., Daruvar, A. de, Dehoux, P., Domann, E., Domínguez-Bernal, G., Duchaud, E., Durant, L., Dussurget, O., Entian, K.-D., Fsihi, H., Portillo, F.G., Garrido, P.,

Gautier, L., Goebel, W., Gómez-López, N., Hain, T., Hauf, J., Jackson, D., Jones, L.-M., Kaerst, U., Kreft, J., Kuhn, M., Kunst, F., Kurapkat, G., Madueno, E., Maitournam, A., Vicente, J.M., Ng, E., Nedjari, H., Nordsiek, G., Novella, S., Pablos, B. de, Pérez-Diaz, J.-C., Purcell, R., Remmel, B., Rose, M., Schlueter, T., Simoes, N., Tierrez, A., Vázquez-Boland, J.-A., Voss, H., Wehland, J., Cossart, P., 2001. Comparative genomics of *Listeria* Species. Science 294 (1979), 849–852. https://doi.org/10.1126/SCIENCE.1063447.

Goncheva, M.I., Flannagan, R.S., Heinrichs, D.E., 2020. De novo purine biosynthesis is required for intracellular growth of *Staphylococcus aureus* and for the hypervirulence phenotype of a purr mutant. Infect. Immun. 88. https://doi.org/10.1128/IAI.00104-20.

Guerreiro, D.N., Arcari, T., O'Byrne, C.P., 2020a. The σB-mediated general stress response of *Listeria monocytogenes*: life and death decision making in a pathogen. Front. Microbiol. 11, 556640. https://doi.org/10.3389/fmicb.2020.01505.

Guerreiro, D.N., Wu, J., Dessaux, C., Oliveira, A.H., Tiensuu, T., Gudynaite, D., Marinho, C.M., Boyd, A., del Portillo, F.G., Johansson, J., O'Byrne, C.P., 2020b. Mild stress conditions during laboratory culture promote the proliferation of mutations that negatively affect sigma B activity in *Listeria monocytogenes*. J. Bacteriol. 202. https://doi.org/10.1128/JB.00751-19.

Hoffman, J.A., Badger, J.L., Zhang, Y., Sik Kim, K., 2001. Escherichia coli K1 pur A and sor C are preferentially expressed upon association with human brain microvascular endothelial cells. Microb. Pathog. 31, 69–79. https://doi.org/10.1006/MPAT.2001.0451.

Hu, F., Zhang, Y., Liu, Q., Wang, Z., 2022. PurA facilitates Edwardsiella piscicida to escape NF-κB signaling activation. Fish. Shellfish Immunol. 124, 254–260. https://doi.org/10.1016/J.FSI.2022.04.001.

Ivánovics, G., Marjai, E., Dobozy, A., 1968. The growth of purine mutants of *Bacillus anthracis* in the body of the mouse. J. Gen. Microbiol. 53, 147–162. https://doi.org/10.1099/00221287-53-2-147.

Jonquières, R., Bierne, H., Fiedler, F., Gounon, P., Cossart, P., 1999. Interaction between the protein InlB of *Listeria monocytogenes* and lipoteichoic acid: a novel mechanism of protein association at the surface of Gram-positive bacteria. Mol. Microbiol. 34, 902–914. https://doi.org/10.1046/J.1365-2958.1999.01652.X.

Kopeckova, M., Pavkova, I., Stulik, J., 2020. Diverse localization and protein binding abilities of glyceraldehyde-3-phosphate dehydrogenase in pathogenic bacteria: the key to its multifunctionality? Front Cell Infect. Microbiol 10, 89. https://doi.org/10.3389/FCIMB.2020.00089.

Lähteenmäki, K., Edelman, S., Korhonen, T.K., 2005. Bacterial metastasis: the host plasminogen system in bacterial invasion. Trends Microbiol. 13, 79–85. https://doi.org/10.1016/J.TIM.2004.12.003.

Lampe, D.J., Churchill, M.E.A., Robertson, H.M., 1996. A purified mariner transposase is sufficient to mediate transposition in vitro. EMBO J. 15, 5470–5479. https://doi.org/10.1002/J.1460-2075.1996.TB00930.X.

Lampe, D.J., Grant, T.E., Robertson, H.M., 1998. Factors affecting transposition of the Himar1 mariner transposon in vitro. Genetics 149, 179–187. https://doi.org/10.1093/GENETICS/149.1.179.

Lan, L., Cheng, A., Dunman, P.M., Missiakas, D., He, C., 2010. Golden pigment production and virulence gene expression are affected by metabolisms in *Staphylococcus aureus*. J. Bacteriol. 192, 3068–3077. https://doi.org/10.1128/JB.00928-09.

Ledala, N., Pearson, S.L., Wilkinson, B.J., Jayaswal, R.K., 2007. Molecular characterization of the Fur protein of *Listeria monocytogenes*. Microbiology 153, 1103–1111. https://doi.org/10.1099/MIC.0.2006/000620-0.

Lipkow, K., Buisine, N., Chalmers, R., 2004. Promiscuous target interactions in the mariner transposon himar1. J. Biol. Chem. 279, 48569–48575. https://doi.org/10.1074/jbc.M408759200.

Liu, X., Kimmey, J.M., Matarazzo, L., de Bakker, V., Van Maele, L., Sirard, J.C., Nizet, V., Veening, J.W., 2021. Exploration of bacterial bottlenecks and *Streptococcus pneumoniae* pathogenesis by CRISPRi-Seq. Cell Host Microbe 29, 107–120.e6. https://doi.org/10.1016/J.CHOM.2020.10.001.

Ma, J., Cai, X., Bao, Y., Yao, H., Li, G., 2018. Uropathogenic *Escherichia coli* preferentially utilize metabolites in urine for nucleotide biosynthesis through salvage pathways. Int. J. Med. Microbiol. 308, 990–999. https://doi.org/10.1016/J.IJMM.2018.08.006.

Marquis, H., Hager, E.J., 2000. pH-regulated activation and release of a bacteria-associated phospholipase C during intracellular infection by *Listeria monocytogenes*. Mol. Microbiol. 35, 289–298. https://doi.org/10.1046/J.1365-2958.2000.01708.X.

McFarland, W.C., Stocker, B.A.D., 1987. Effect of different purine auxotrophic mutations on mouse-virulence of a Vi-positive strain of *Salmonella* dublin and of two strains of *Salmonella typhimurium*. Micro Pathog. 3, 129–141. https://doi.org/10.1016/0882-4010(87)90071-4.

Mengaud, J., Lecuit, M., Lebrun, M., Nato, F., Mazie, J.C., Cossart, P., 1996. Antibodies to the leucine-rich repeat region of internalin block entry of *Listeria monocytogenes* into cells expressing E-cadherin. Infect. Immun. 64, 5430. https://doi.org/10.1128/IAI.64.12.5430-5433.1996.

Milohanic, E., Pron, B., Berche, P., Gaillard, J.L., Glaser, P., Amend, A., Baquero-Mochales, F., Bloecker, H., Brandt, P., Buchrieser, C., Chakraborty, T., Charbit, A., Couvé, E., De Daruvar, A., Dehoux, P., Domann, E., Dominguez-Bernal, G., Durand, L., Entian, K.D., Frangeul, L., Fsihi, H., Garcia Del Portillo, F., Garrido, P., Goebel, W., Gomez-Lopez, N., Hain, T., Hauf, J., Jackson, D., Kreft, J., Kunst, F., Mata-Vicente, J., Ng, E., Nordsiek, G., Perez-Diaz, J.C., Remmel, B., Rose, M., Rusniok, C., Schlueter, T., Vazquez-Boland, J.A., Voss, H., Wehland, J., Cossart, P., 2000. Identification of new loci involved in adhesion of *Listeria monocytogenes* to eukaryotic cells. Microbiology 146, 731–739. https://doi.org/10.1099/00221287-146-3-731.

Monk, I.R., Gahan, C.G.M., Hill, C., 2008. Tools for functional postgenomic analysis of *Listeria monocytogenes*. Appl. Environ. Microbiol. 74, 3921–3934. https://doi.org/10.1128/AEM.00314-08.

Narayanan, L., Ozdemir, O., Alugubelly, N., Ramachandran, R., Banes, M., Lawrence, M., Abdelhamed, H., 2022. Identification of genetic elements required for *Listeria monocytogenes* growth under limited nutrient conditions and virulence by a screening of transposon insertion library. Front. Microbiol. 13, 1007657. https://doi.org/10.3389/FMICB.2022.1007657.

Nowak, J., Visnovsky, S.B., Pitman, A.R., Cruz, C.D., Palmer, J., Fletcher, G.C., Flint, S., 2021. Biofilm formation by *Listeria monocytogenes* 15G01, a persistent isolate from a seafood-processing plant, is influenced by inactivation of multiple genes belonging to different functional groups. Appl. Environ. Microbiol 87, 1–19. https://doi.org/10.1128/AEM.02349-20.

Oliver, H.F., Orsi, R.H., Wiedmann, M., Boor, K.J., 2010. *Listeria monocytogenes* σB has a small core regulon and a conserved role in virulence but makes differential contributions to stress tolerance across a diverse collection of strains. Appl. Environ. Microbiol. 76, 4216–4232. https://doi.org/10.1128/AEM.00031-10.

Osanai, A., Li, S.J., Asano, K., Sashinami, H., Hu, D.L., Nakane, A., 2013. Fibronectin-binding protein, FbpA, is the adhesin responsible for pathogenesis of *Listeria monocytogenes* infection. Microbiol. Immunol. 57, 253–262. https://doi.org/10.1111/1348-0421.12030.

Pang, X., Wu, Yansha, Liu, X., Wu, Yajing, Shu, Q., Niu, J., Chen, Q., Zhang, X., 2022. The lipoteichoic acid-related proteins YqgS and LafA contribute to the resistance of *Listeria monocytogenes* to Nisin. Microbiol. Spectr. 10. https://doi.org/10.1128/SPECTRUM.02095-21.

Park, S.F., Stewart, G.S.A.B., 1990. High-efficiency transformation of *Listeria monocytogenes* by electroporation of penicillin-treated cells. Gene 94, 129–132. https://doi.org/10.1016/0378-1119(90)90479-B.

Parsons, C., Lee, S., Jayeola, V., Kathariou, S., 2017. Novel cadmium resistance determinant in *Listeria monocytogenes*. Appl. Environ. Microbiol. 83. https://doi.org/10.1128/AEM.02580-16.

Paspaliari, D.K., Kastbjerg, V.G., Ingmer, H., Popowsk, M., Larsen, M.H., 2017. Chitinase expression in *Listeria monocytogenes* is influenced by lmo0327, which encodes an internalin-like protein. Appl. Environ. Microbiol. 83. https://doi.org/10.1128/AEM.01283-17.

Peetermans, M., Vanassche, T., Liesenborghs, L., Lijnen, R.H., Verhamme, P., 2016. Bacterial pathogens activate plasminogen to breach tissue barriers and escape from innate immunity. Crit. Rev. Microbiol. 42, 866–882. https://doi.org/10.3109/1040841X.2015.1080214.

Pillich, H., Puri, M., Chakraborty, T., 2017. ActA of *Listeria monocytogenes* and its manifold activities as an important listerial virulence factor. Curr. Top. Microbiol. Immunol. 399, 113–132. https://doi.org/10.1007/82_2016_30.

Pizarro-Cerdá, J., Kühbacher, A., Cossart, P., 2012. Entry of *Listeria monocytogenes* in mammalian epithelial cells: an updated view. Cold Spring Harb. Perspect. Med. 2, a010009. https://doi.org/10.1101/CSHPERSPECT.A010009.

Polissi, A., Pontiggia, A., Feger, G., Altieri, M., Mottl, H., Ferrari, L., Simon, D., 1998. Large-scale identification of virulence genes from *Streptococcus pneumoniae*. Infect. Immun. 66, 5620–5629. https://doi.org/10.1128/IAI.66.12.5620-5629.1998.

Pöntinen, A., Markkula, A., Lindström, M., Korkeala, H., 2015. Two-component-system histidine kinases involved in growth of *Listeria monocytogenes* EGD-e at low temperatures. Appl. Environ. Microbiol. 81, 3994–4004. https://doi.org/10.1128/AEM.00626-15.

Radoshevich, L., Cossart, P., 2017. *Listeria monocytogenes*: towards a complete picture of its physiology and pathogenesis, 2017 16:1 Nat. Rev. Microbiol. 16, 32–46. https://doi.org/10.1038/nrmicro.2017.126.

Ray, K., Marteyn, B., Sansonetti, P.J., Tang, C.M., 2009. Life on the inside: the intracellular lifestyle of cytosolic bacteria, 2009 7:5 Nat. Rev. Microbiol. 7, 333–340. https://doi.org/10.1038/nrmicro2112.

Rea, R.B., Gahan, C.G.M., Hill, C., 2004. Disruption of putative regulatory loci in *Listeria monocytogenes* demonstrates a significant role for fur and PerR in virulence. Infect. Immun. 72, 717–727. https://doi.org/10.1128/IAI.72.2.717-727.2004.

Reis, O., Sousa, S., Camejo, A., Villiers, V., Gouin, E., Cossart, P., Cabanes, D., 2010. LapB, a novel *Listeria monocytogenes* LPXTG surface adhesin, required for entry into eukaryotic cells and virulence. J. Infect. Dis. 202, 551–562. https://doi.org/10.1086/654880.

Reniere, M.L., Whiteley, A.T., Hamilton, K.L., John, S.M., Lauer, P., Brennan, R.G., Portnoy, D.A., 2015. Glutathione activates virulence gene expression of an intracellular pathogen, 2015 517:7533 Nature 517, 170–173. https://doi.org/10.1038/nature14029.

Schauer, K., Geginat, G., Liang, C., Goebel, W., Dandekar, T., Fuchs, T.M., 2010. Deciphering the intracellular metabolism of *Listeria monocytogenes* by mutant screening and modelling. BMC Genom. 11, 573. https://doi.org/10.1186/1471-2164-11-573.

Schlech, W.F., 2019. Epidemiology and clinical manifestations of *Listeria monocytogenes* infection. Microbiol. Spectr. 7. https://doi.org/10.1128/MICROBIOLSPEC.GPP3-0014-2018.

Sleator, R.D., Gahan, C.G.M., Hill, C., 2001. Identification and disruption of the proBA Locus in *Listeria monocytogenes:* role of proline biosynthesis in salt tolerance and murine infection. Appl. Environ. Microbiol. 67, 2571–2577. https://doi.org/10.1128/AEM.67.6.2571-2577.2001.

Sleator, R.D., Hill, C., 2005. A novel role for the LisRK two-component regulatory system in listerial osmotolerance. Clin. Microbiol. Infect. 11, 599–601. https://doi.org/10.1111/J.1469-0691.2005.01176.X.

Smith, G.A., Marquis, H., Jones, S., Johnston, N.C., Portnoy, D.A., Goldfine, H., 1995. The two distinct phospholipases C of *Listeria monocytogenes* have overlapping roles in

escape from a vacuole and cell-to-cell spread. Infect. Immun. 63, 4231–4237. https://doi.org/10.1128/IAI.63.11.4231-4237.1995.

Sun, Y., Fukamachi, T., Saito, H., Kobayashi, H., 2011. Atp requirement for acidic resistance in *Escherichia coli*. J. Bacteriol. 193, 3072–3077. https://doi.org/10.1128/JB.00091-11.

Tsai, H.N., Hodgson, D.A., 2003. Development of a synthetic minimal medium for *Listeria monocytogenes*. Appl. Environ. Microbiol 69, 6943–6945. https://doi.org/10.1128/AEM.69.11.6943-6945.2003.

Vessey, C.J., Wilding, J., Folarin, N., Hirano, S., Takeichi, M., Soutter, P., Stamp, G.W.H., Pignatelli, M., 1995. Altered expression and function of E-cadherin in cervical intraepithelial neoplasia and invasive squamous cell carcinoma. J. Pathol. 176, 151–159. https://doi.org/10.1002/PATH.1711760208.

Winterbourn, C.C., Peskin, A.V., Kleffmann, T., Radi, R., Pace, P.E., 2023. Carbon dioxide/bicarbonate is required for sensitive inactivation of mammalian glyceraldehyde-3-phosphate dehydrogenase by hydrogen peroxide. Proc. Natl. Acad. Sci. USA 120, e2221047120. https://doi.org/10.1073/PNAS.2221047120.

Zemansky, J., Kline, B.C., Woodward, J.J., Leber, J.H., Marquis, H., Portnoy, D.A., 2009. Development of a mariner-based transposon and identification of *Listeria monocytogenes* determinants, including the peptidyl-prolyl isomerase PrsA2, that contribute to its hemolytic phenotype. J. Bacteriol. 191, 3950–3964. https://doi.org/10.1128/JB.00016-09.